1969

A comparison of lumped parameter models commonly used to describe one-dimensional vibration problems

Suresh Kumar Tolani

Department:

A COMPARISON OF LUMPED PARAMETER MODELS COMMONLY USED TO DESCRIBE ONE-DIMENSIONAL VIBRATION PROBLEMS

By

SURESH KUMAR TOLANI, (1946)-

A

THESIS

submitted to the faculty of

UNIVERSITY OF MISSOURI - ROLLA

in partial fulfillment of the requirements for the

Degree of

MASTER OF SCIENCE IN MECHANICAL ENGINEERING

Rolla, Missouri

1969

Approved by

Richard D Rocke (advisor) Clark L Barker

Floyd M. Cunningham

ABSTRACT

Three lumped parameter model representations of the one-dimensional uniform continuous system in a vibration state are examined. The exact (continuous) solutions were used as a reference to evaluate the accuracy of the results obtained via these discrete element models.

The model comparisons, carried out for both the principal modes and the systems under forced excitations, are based on the maximum strain energy. The effect of varying the number of segments in the model representation showed improvement in approximating the exact strain energy solution as the number of segments was increased.

In general, the results of the model comparisons based on maximum strain energy were consistent with previous comparisons made on the basis of frequency root errors.

ACKNOWLEDGEMENTS

The author desires to gratefully acknowledge the guidance and encouragement given by his advisor, Dr. Richard D. Rocke, in the preparation of this manuscript. The author is further indebted to the National Science Foundation for the financial aid provided through the University of Missouri - Rolla in support of this work. Thanks are also extended to Mrs. Judy Guffey for typing this manuscript.

TABLE OF CONTENTS

LIST OF ILLUSTRATIONS

LIST OF TABLES

NOMENCLATURE

A_o = Peak base acceleration

E = Modulus of elasticity

$f_\nu(t)$ = Time dependent part of the displacement function in the νth mode

$f_{nR}(t)$ = Time dependent part of the relative displacement function in the nth mode

$\ddot{f}_{nR}(t) = \dfrac{d^2 f_{nR}(t)}{dt^2}$

GJ = Torsional stiffness per unit length

K = Spring stiffness

$[K]$ = Stiffness matrix

l = Length of each segment of the bar

L = Length of the rod

m = Mass of each segment of the rod

$[m]$ = Diagonal mass matrix

M = Total mass of the rod

N = Number of segments

$\{P\}$ = Principal coordinate vector

r = Gas constant

t = Time

πt_1 = Half sine pulse duration time

T_1 = Absolute temperature of the gas in ^oK

$\ddot{u}_B(t)$ = General time varying base acceleration

U_c = Strain energy of the continuous system

U_m = Strain energy of the model

$U_\nu(x)$ = νth mode shape function

$U_{nR}(x)$ = nth mode shape in the relative coordinate

$U'_{nR}(x) = \frac{dU_{nR}(x)}{dx}$

$U''_{nR}(x) = \frac{d^2U_{nR}(x)}{dx^2}$

$\{x\}$ = Eigenvectors of the model

$\{\tilde{x}\}$ = Relative coordinate vector

$\bar{X_N}$ = Maximum displacement at the Nth mass in the model

γ = Ratio of specific heat of the gas at constant pressure to that at constant volume

θ = Angular displacement of the shaft

ν = Mode number = 1, 2, 3, ...(all positive integers)

ρ = Mass per unit length of the rod

σ = Stress

τ = Time

ω_ν = Circular frequency in the νth mode

CHAPTER I

INTRODUCTION

A general theory for solving vibration problems involving continuous systems has been in existence for many years. However, the number of problems which can be solved analytically is very small. Therefore, other techniques which give approximate solutions to continuous systems, have been extensively investigated.

One such technique, which has been very popular since the advent of large computers, is the lumped parameter model approximation. Here the continuum is replaced by a finite N degree-of-freedom system composed of lumped elements, i.e., massless springs, point masses, etc. This technique actually dates back to the fundamental work in vibration by Lagrange and Rayleigh. Duncan[1], using the same technique, was one of the first to study the behavior of errors in frequency roots resulting from the lumped parameter model approximation. Other investigators have also used the frequency root error comparison for models ranging from rods and bars to beams and plate elements.

Rocke[2] has compared lumped parameter models for the one-dimensional systems, i.e., vibrating systems which are governed by the one-dimensional wave equation, using the same basis of comparison and has attempted to evaluate whether those models, which are judged best on the basis of smaller frequency root errors, do indeed provide better dynamic description under general transient type behavior. The cases

treated by Rocke include only the constant base acceleration excitation of rods and beams and because of inconsistent results his work points out the necessity of having a consistent basis of comparison.

The work presented herein attempts to provide a consistent basis of comparison for lumped parameter models of one-dimensional systems in a general dynamic state. The basis to be used is the maximum strain energy of the system. Strain energy is proportional to the stress times the strain in the system and summed over the entire system. Hence, it should be indicative of displacements and stresses in the system independent of their position within the system. Furthermore, the maximum system strain energy should be a better measure of total system distortion than any one particular parameter, e.g., maximum displacement or maximum stress.

A. Contents of Thesis

Chapter II contains a description of the one-dimensional uniform continuous systems. The governing differential equation and its homogeneous solutions have been established. To study the system under forced excitation, a constant base acceleration type of excitation has been used to verify the analytical solutions derived and to study the behavior of the models on the basis of maximum system strain energy. A half sine pulse base acceleration type of excitation has also been examined to include a time-varying forced excitation. The period of the half sine pulse has been varied to

be less than, greater than, and nearly equal to the fundamental period of the system.

The base acceleration excitation when using relative coordinates is analogous to the case of a distributed forcing function, which is only a function of time and not of position, imposed upon the uniform one-dimensional system with fixed base and absolute coordinates. The latter has not been studied directly since it is covered by the former type of excitation.

Strain energy of the continuous systems, which is used as a reference for the comparison of the lumped parameter models, has also been established in closed form in Chapter II for the systems in both the principal modes and the general transient state for base excitations described.

Chapter III describes the three lumped parameter models used to describe the continuous one-dimensional systems. Evaluation of the models as they approximate the continuous systems has been made. Strain energy for both the principal modes and the forced excitation conditions has been established using matrix algebra.

In Chapter IV, comparisons of the models have been made on the basis of the maximum system strain energy to determine if any given model is best. Use of an IBM-360-50 computer has been made to establish numerical results for the maximum system strain energy of the various cases. These comparisons, based on the maximum system strain energy, have been made for both the principal modes and the forced excitation response.

To check the validity of the solutions established for the system strain energy, the results for maximum displacement and maximum stress were compared with those of Rocke[2] for the case of constant base acceleration. A half sine pulse base acceleration was used to study the effect of time-varying excitations on the evaluation of the models.

CHAPTER II

CONTINUOUS SYSTEMS

A. Governing Differential Equations

Systems represented by the one-dimensional wave equation, i.e., longitudinal vibrations of bars, torsional oscillations of shafts, transverse vibrations of strings, acoustical oscillations in ducts, etc., are of practical importance in engineering design problems. Once the one-dimensional wave equation, as it governs these various systems, is established and its general solution found all solutions to the above systems are determined within applicable constants. To illustrate the derivation of the one-dimensional wave equation the cases of the longitudinal rod and torsional bar will be used.

Figure 1 shows a thin uniform bar. Because of axial forces there will be a displacement 'u' of any particular point along the bar which will be a function of both the particle's position 'x' and time 't'. Since the bar has a continuous distribution of mass and stiffness it has an infinite number of natural modes of vibration and the displacement of any given cross section will differ with each mode.

Considering a 'dx' element of this bar, it is evident that the element in the new position has changed in length by an amount $\frac{\partial u}{\partial x}\ dx$; thus, the unit strain is $\frac{\partial u}{\partial x}$. Using Newton's law of motion and equating the unbalanced force on the element to the product of the mass and the average acceleration of the element gives:

$$\frac{\partial P}{\partial x}\ dx = \rho\ dx\ \frac{\partial^2 u}{\partial t^2}\ , \text{ or}$$

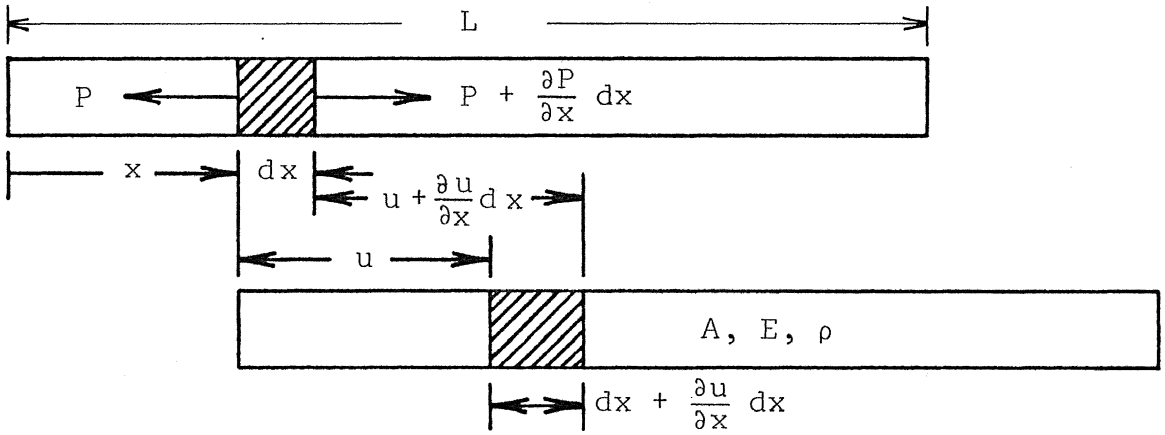

Fig. 1 Displacement of a Uniform Continuous Rod Element

$$\frac{\partial P}{\partial x} = \rho \frac{\partial^2 u}{\partial t^2} . \qquad (2.1)$$

From Hooke's law the ratio of unit stress to unit strain is equal to the modulus of elasticity E. Thus,

$$\frac{P/A}{(\partial u/\partial x)} = E$$

where: A is the cross-sectional area of the bar.

Differentiating this expression with respect to x gives:

$$\frac{\partial P}{\partial x} = AE \frac{\partial^2 u}{\partial x^2} . \qquad (2.2)$$

From eqs. (2.1) and (2.2)

$$AE \frac{\partial^2 u}{\partial x^2} = \rho \frac{\partial^2 u}{\partial t^2} , \text{ or}$$

$$\frac{\partial^2 u}{\partial t^2} = \frac{AE}{\rho} \frac{\partial^2 u}{\partial x^2} .$$

Defining,

$$AE/\rho = a^2$$

the governing differential equation becomes:

$$\frac{\partial^2 u}{\partial t^2} = a^2 \frac{\partial^2 u}{\partial x^2} \qquad (2.3)$$

where a^2 is a system constant and depends on the physical properties of the system as will be illustrated by considering a second, but different system.

Figure 2 shows torques on a 'dx' element of a uniform bar in torsion. In the derivation of the governing differential equation for the torsional vibration of shafts, the approach is the same as explained for the longitudinal

vibration of rods except that forces 'P' and the longitudinal displacement 'u' in the latter case are replaced by the torques 'T' and the angular displacement 'θ', respectively.

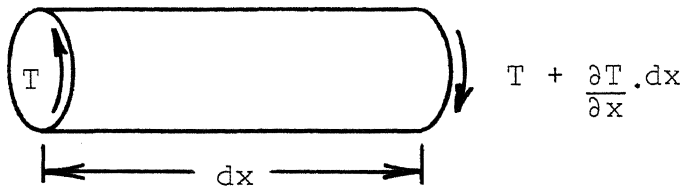

Fig. 2 Torque Acting on a 'dx' Element of a shaft

Therefore, Newton's law of motion for this system gives:

$$\frac{\partial T}{\partial x}\, dx = I_p\, dx\, \frac{\partial^2 \theta}{\partial t^2}\ , \text{ or}$$

$$\frac{\partial T}{\partial x} = I_p\, \frac{\partial^2 \theta}{\partial t^2} \qquad (2.4)$$

where: I_p = mass moment of inertia per unit length of the rod.

The angle of twist for the element dx is given by,

$$\partial\theta = \frac{T\partial x}{GJ}\ , \text{ or}$$

$$\frac{\partial \theta}{\partial x} = \frac{T}{GJ}\ .$$

$$\therefore \quad GJ\, \frac{\partial^2 \theta}{\partial x^2} = \frac{\partial T}{\partial x} \qquad (2.5)$$

From eqs. (2.4) and (2.5),

$$\frac{\partial^2 \theta}{\partial t^2} = \frac{GJ}{I_p}\, \frac{\partial^2 \theta}{\partial x^2}\ , \text{ or}$$

$$\frac{\partial^2 \theta}{\partial t^2} = a^2 \frac{\partial^2 \theta}{\partial x^2} \qquad (2.6)$$

where: $a^2 = GJ/I_p$.

It may be noted here that eqs. (2.3) and (2.6) are similar except for the constant 'a'. Similarly, the partial differential equation of motion for other one-dimensional systems is the same as eq. (2.3) except for the change in constant 'a'. Table I shows the values of the constant a^2 for various one-dimensional systems.

Table I

Constant "a^2" for Various One-dimensional Systems

TYPE OF SYSTEM	a^2
Longitudinal vibration of bars	AE/ρ
Torsional oscillations of shafts	GJ/I_p
Acoustical oscillations of tubes	$\gamma r T_1$
Transverse vibrations of strings	S/ρ

Solution of eq. (2.3) is, therefore, applicable to all the above systems and others within the constants or parameters which are basic to that system's description with eq. (2.3).

B. Homogeneous Solutions

Using a standard separation of variables solution of the form,

$$u(x,t) = U(x)\, f(t)$$

eq. (2.3) becomes:

$$U(x)\,\frac{\partial^2 f(t)}{\partial t^2} = a^2 f(t)\,\frac{\partial^2 U(x)}{\partial x^2}\ , \text{ or}$$

$$\frac{1}{f(t)}\,\frac{\partial^2 f(t)}{\partial t^2} = a^2\,\frac{1}{U(x)}\,\frac{\partial^2 U(x)}{\partial x^2}\ . \qquad (2.7)$$

Since the left hand side of eq. (2.7) is independent of x and the right hand side is independent of t, it follows that each side must be equal to a constant. Assuming that both sides of this equation are equal to $-\omega^2$, two differential equations can be obtained:

$$\frac{d^2 U(x)}{dx^2} + \left(\frac{\omega}{a}\right)^2 U(x) = 0 \qquad (2.8)$$

$$\frac{d^2 f(t)}{dt^2} + \omega^2 f(t) = 0\ . \qquad (2.9)$$

General solutions of these two differential equations are given by:

$$U(x) = C\cos\left(\frac{\omega}{a}x\right) + D\sin\left(\frac{\omega}{a}x\right) \qquad (2.10)$$

$$f(t) = A\cos(\omega t) + B\sin(\omega t)\ . \qquad (2.11)$$

The arbitrary constants A, B and C, D depend on the initial conditions and the boundary conditions, respectively.

It is of interest to note that if the constant chosen for eq. (2.7) was $+\omega^2$, the time dependent part of the solution f(t), is given by:

$$f(t) = A\cosh(\omega t) + B\sinh(\omega t)$$

which does not provide an oscillatory solution, as being sought. The total solution from eqs. (2.10) and (2.11) becomes:

$$u(x,t) = [A \cos(\omega t) + B \sin(\omega t)] \; [C \cos(\frac{\omega}{a} x) + D \sin(\frac{\omega}{a} x)] \; . \tag{2.12}$$

This homogeneous solution is applicable to all the one-dimensional systems except for the change in the value of constant 'a'. For simplicity the longitudinal rod will be the common system of reference in this study and all equations and solutions will reflect the appropriate constants and parameters for this system. Hence, to apply the solutions herein to any one-dimensional system requires a change in appropriate physical constant only. Likewise, any comparison of lumped parameter models should be invariant to any physical system.

B.1 Homogeneous Solutions with Various Boundary Conditions

For one-dimensional systems there can be four sets of possible boundary conditions considering free and fixed ends, i.e., fixed-fixed, free-free, fixed-free and free-fixed. Previous work[2] has shown that the behavior of the system for the fixed-fixed and free-free end conditions is similar while that of fixed-free ends is physically a mere image of the free-fixed case. This reduces further investigation to only two of the four sets of boundary conditions, i.e., fixed-fixed and fixed-free. In this report these end conditions have been chosen and used throughout.

The mode shapes depend on the specific boundary conditions and can be obtained by using eq. (2.10), which is:

$$U(x) = C \cos(\frac{\omega}{a} x) + D \sin(\frac{\omega}{a} x) \; .$$

Fixed-Fixed ends:

These boundary conditions require the following restrictions on the spatial function:

$$u(0,t) = 0 \text{ and } u(L,t) = 0 \ .$$

Since $u(x,t) = U(x)\ f(t)$, it follows that

$$U(0) = C = 0, \text{ and}$$

$$U(L) = D \sin(\frac{\omega}{a})\ L = 0 \ .$$

D cannot be equal to zero since the resulting trivial solution $U(x) = 0$, which implies no vibrations, would be obtained. Therefore, for vibrations to occur:

$$\text{Sin}(\frac{\omega}{a}\ L) = 0, \text{ or}$$

$$\frac{\omega}{a}\ L = \nu\pi \ . \qquad (2.13)$$

where: ν = mode number = $1,2,3,4,.....,\infty$

L and a are constants, independent of the mode number. Therefore, eq. (2.13) shows that the natural frequency depends on the mode number and should be subscripted to each mode, i.e.,

$$(\frac{\omega_\nu}{a})\ L = \nu\pi, \text{ or}$$

$$(\frac{\omega_\nu}{a}) = \frac{\nu\pi}{L} \ .$$

Thus, the mode shapes for fixed-fixed ends are given by:

$$U_\nu(x) = D_\nu \sin(\frac{\omega_\nu}{a})\ x, \text{ or}$$

$$U_\nu(x) = D_\nu \sin(\frac{\nu\pi}{L})\ x \qquad (2.14)$$

where: D_ν = a normalization constant.

Fixed-Free boundary conditions:

The fixed end condition at x = 0 requires u(0,t) = 0 which specifies directly that:

$$U(0) = C = 0 \ .$$

The free end condition at x = L requires zero stress at the free end, i.e.,

$$E \left.\frac{\partial u}{\partial x}\right|_{x=L} = 0, \text{ or}$$

$$\left.\frac{\partial u}{\partial x}\right|_{x=L} = 0$$

$$\therefore \quad U'(L) = 0, \text{ since } f(t) \neq 0.$$

$$\therefore \quad U'(L) = D\left(\frac{\omega}{a}\right).\cos\left(\frac{\omega}{a}\right) L = 0 \ .$$

But D and $\left(\frac{\omega}{a}\right)$ cannot be equal to zero for vibrations to occur; therefore,

$$\cos\left(\frac{\omega}{a}\right) L = 0, \text{ or}$$

$$\frac{\omega}{a} L = (2\nu-1)\ \pi/2 \ . \qquad (2.15)$$

where: $\nu = 1,2,3,.....$(all positive integers).

Equation (2.15) shows that ω needs to be subscripted, being dependent on the mode number

$$\therefore \quad \left(\frac{\omega_\nu}{a}\right) = (2\nu-1)\ \pi/2L \ .$$

Thus, the mode shapes for fixed-free ends are given by:

$$U_\nu(x) = D_\nu \sin\ [(2\nu-1)\ \pi x/2L] \qquad (2.16)$$

where: D_ν = a normalization constant.

C. Forced Excitation Solution

Two types of forced excitations have been used to study the model description of the continuum under transient behavior. These are:

(i) constant base acceleration

(ii) half sine pulse base acceleration

Constant base acceleration has been chosen, since some of the previous comparisons[2] have been made using the same type of excitation. These comparisons, based on the maximum system displacement and the maximum system stress, have been reviewed. Furthermore, comparisons of the lumped parameter models have been made on the basis of the maximum system strain energy herein, using constant base acceleration type of excitation. For these comparisons, system strain energy expressions have been evaluated for the one-dimensional continuous systems in this chapter. Maximum system strain energy of the continuous system is used as the reference quantity for the above comparisons.

In the second case, the one-dimensional systems have been considered for four variations of the duration of the half sine pulse. This type of excitation has been included to examine the time-varying forced excitations. The solution for the displacement function for both the constant base acceleration and the half sine pulse base acceleration $u_R(x,t)$ are dealt with in this section of the study.

The boundary conditions used are fixed-free to obtain a consistent comparison between the results using the strain

energy approach and the previous results.

C.1 Constant Base Acceleration Excitation

A constant base acceleration, A_o, is applied at the left end of the rod. In this type of excitation all normal modes are excited, some to a greater extent than others. Also with the constant excitation, the characteristic time (period) of the forcing function is not aligned with any of the normal mode periods.

Figure 3 shows a thin uniform bar with a known base displacement $u_B(t)$ and a base acceleration $\ddot{u}_B(t)$.

Let, $$u(x,t) = u_R(x,t) + u_B(t) \qquad (2.17)$$

where $u_R(x,t)$ is the displacement, at distance x and time t, relative to that of the base of the bar.

Using eq. (2.17) in eq. (2.3) gives:

$$\frac{\partial^2 u_R(x,t)}{\partial t^2} + \ddot{u}_B = a^2 \frac{\partial^2 u_R(x,t)}{\partial x^2} ,$$

since u_B is only a function of time t and not of position x.

$$\therefore \quad \frac{\partial^2 u_R(x,t)}{\partial t^2} = a^2 \frac{\partial^2 u_R(x,t)}{\partial x^2} - \ddot{u}_B . \qquad (2.18)$$

Equation (2.18), now becomes the governing differential equation. It will be shown by applying Newton's law of motion to an element 'dx' shown in fig. 3a that eq. (2.18) is similar to that which represents a system having a distributed forcing function F(t) which is independent of the position 'x'. Equating forces on the 'dx' element in fig. 3a gives:

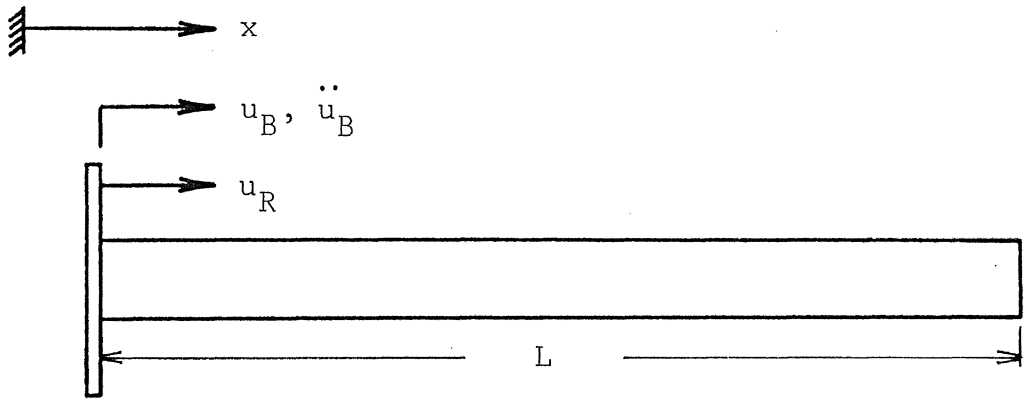

Fig. 3 Continuous Bar with Base Acceleration $\ddot{u}_B(t)$

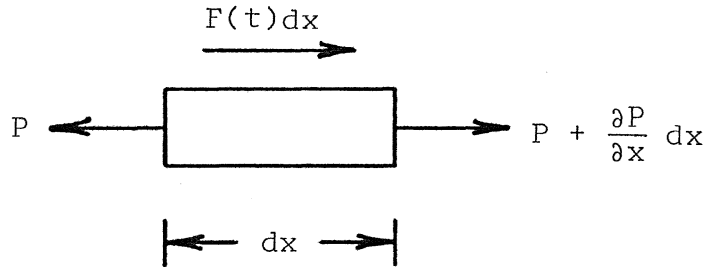

Fig. 3a 'dx' Element with Uniformly Distributed Force F(t)

$$\frac{\partial P}{\partial x}\,dx + F(t)\,dx = \rho\,dx\,\frac{\partial^2 u}{\partial t^2}\ , \text{ or}$$

$$\frac{\partial P}{\partial x} = \rho\,\frac{\partial^2 u}{\partial t^2} - F(t)\ .$$

From eq. (2.2)

$$\frac{\partial P}{\partial x} = AE\,\frac{\partial^2 u}{\partial x^2}$$

combining the above two equations,

$$AE\,\frac{\partial^2 u}{\partial x^2} = \rho\,\frac{\partial^2 u}{\partial t^2} - F(t)\ , \text{ or}$$

$$\frac{\partial^2 u}{\partial t^2} = a^2\,\frac{\partial^2 u}{\partial x^2} + \frac{F(t)}{\rho} \text{ is obtained.}$$

This is similar to eq. (2.18) except that $\ddot{u}_B$ has been replaced by $-F(t)/\rho$. Hence, all solutions and conclusions derived herein are also valid for a fixed base system with a time-dependent uniformly distributed forcing function F(t).

Solution of eq. (2.18) can be obtained by the standard procedure of separation of variables. Earlier, it has been shown that there exists an infinite number of principal modes and solutions. Thus, the most general solution would then be the summation of all of these solutions. Therefore, the form of the solution for eq. (2.18) can be given by:

$$u_R(x,t) = \sum_{n=1}^{\infty} U_{nR}(x)\ f_{nR}(t) \qquad (2.19)$$

where $U_{nR}(x)$ are the mode shapes of the bar relative to its base and $f_{nR}(t)$ is the accompanying time dependent part of the solution. Substituting eq. (2.19) into eq. (2.18) gives:

$$\sum_{n=1}^{\infty} U_{nR}(x)\, \ddot{f}_{nR}(t) = a^2 \sum_{n=1}^{\infty} U''_{nR}(x)\, f_{nR}(t) - \ddot{u}_B .$$

Multiplying each side by $U_{mR}(x)\,dx$ and integrating from 0 to L,

$$\int_0^L \sum_{n=1}^{\infty} U_{nR}(x)\, U_{mR}(x)\, \ddot{f}_{nR}(t)\, dx$$

$$= a^2 \int_0^L \sum_{n=1}^{\infty} U''_{nR}(x)\, U_{mR}(x)\, f_{nR}(t)\, dx - \int_0^L \ddot{u}_B\, U_{mR}(x)\, dx$$

$$= a^2 \cdot \sum_{n=1}^{\infty} \left[\left(U'_{nR}(x)\, U_{mR}(x) \Big|_0^L - \int_0^L U'_{nR}(x)\, U'_{mR}(x)\, dx \right) f_{nR}(t) \right] - \int_0^L \ddot{u}_B U_{mR}(x)\, dx$$

is obtained.

It should be noted here that the first term on the right hand side, when evaluated at x = 0 or x = L, is always zero since $U'_{nR}(x=L) = U_{mR}(x=0) = 0$ for the fixed-free ends.

$$\therefore \quad \sum_{n=1}^{\infty} \int_0^L U_{nR}(x)\, U_{mR}(x)\, \ddot{f}_{nR}(t)\, dx = - a^2 \sum_{n=1}^{\infty} \int_0^L U'_{nR}(x)\, U'_{mR}(x)\, f_{nR}(t)\, dx - \int_0^L \ddot{u}_B\, U_{mR}(x)\, dx \, . \qquad (2.20)$$

The orthogonality and normalization relationships are given by:

$$\int_0^L \rho\, U_{nR}(x)\, U_{mR}(x)\, dx = \begin{cases} 0 , & m \neq n \\ \int_0^L \rho\, U_{nR}^2(x)\, dx , & m = n \end{cases} \qquad (2.21)$$

and,

$$\int_0^L \rho\, U'_{nR}(x)\, U'_{mR}(x)\, dx = 0 , \qquad m \neq n \tag{2.22}$$

$$= \int_0^L \rho \left[U'_{nR}(x)\right]^2 . dx, \quad m = n .$$

Using eqs. (2.21) and (2.22) in eq. (2.20) gives:

$$\int_0^L U_{nR}{}^2(x)\, \ddot{f}_{nR}(t)\, dx = -a^2 \int_0^L \{U'_{nR}(x)\}^2\, f_{nR}(t)\, dx$$

$$-\int_0^L \ddot{u}_B\, U_{nR}(x)\, dx, \text{ or}$$

$$\left[\int_0^L U_{nR}{}^2(x)\, dx\right] \ddot{f}_{nR}(t) + a^2 \left[\int_0^L \{U'_{nR}(x)\}^2\, dx\right] f_{nR}(t)$$

$$= -\int_0^L \ddot{u}_B\, U_{nR}(x)\, dx$$

$$= -\ddot{u}_B \int_0^L U_{nR}(x)\, dx .$$

Referring back to the classical free vibration analysis discussed in section B, for the fixed-free boundary conditions,

$$U_{nR}(x) = D_{nR} \sin(n\pi x/2L), \quad n=1,3,5,.... \tag{2.24}$$

where: D_{nR} = a normalization constant.

The normalization constant, D_{nR}, is found by equating the normalization relation to the total mass of the bar, or,

$$\int_0^L \rho . U_{nR}{}^2(x)\, dx = \rho L , \text{ or}$$

$$D_{nR}{}^2 = L \Big/ \int_0^L \sin^2(n\pi x/2L)\, dx .$$

$$\therefore \quad D_{nR} = \sqrt{2} \quad , \text{ and}$$

$$U_{nR}(x) = \sqrt{2}\, \sin(n\pi x/2L) \ . \qquad (2.25)$$

Substituting for $U_{nR}(x)$ from eq. (2.25) into eq. (2.23) gives:

$$2\left[\int_0^L \sin^2(n\pi x/2L)\, dx\right] \ddot{f}_{nR}(t) + 2a^2 \left[\int_0^L \left(\frac{n\pi}{2L}\right)^2 \cos^2(n\pi x/2L)\, dx\right]$$

$$= -\sqrt{2}\, \ddot{u}_B \int_0^L \sin(n\pi x/2L)\, dx, \text{ or}$$

$$\ddot{f}_{nR}(t) \cdot L/2 + a^2 \left(\frac{n\pi}{2L}\right)^2 \cdot L/2\, f_{nR}(t) = -\frac{\ddot{u}_B}{\sqrt{2}} (2L/n\pi)$$

as $\int_0^L \sin^2(n\pi x/2L)\, dx = \int_0^L \cos^2(n\pi x/2L)\, dx = L/2$.

$$\therefore \quad \ddot{f}_{nR}(t) + \omega_{nR}^2\, f_{nR}(t) = F(t) \qquad (2.26)$$

where: $F(t) = -2\sqrt{2}\, \ddot{u}_B(t)/n\pi$.

This equation is of the form,

$$\ddot{f}_n(t) + \omega_n^2\, f_n(t) = F(t)$$

and by Duhamel's integral solution (with zero initial conditions):

$$f_{nR}(t) = \int_0^L \frac{\sin\left[\omega_{nR}(t-\tau)\right]}{\omega_{nR}} \cdot \frac{-2\sqrt{2}\, \ddot{u}_B(\tau)}{n\pi}\, d\tau. \qquad (2.27)$$

For a constant base acceleration:

$$\ddot{u}_B(t) = A_o = \text{constant (time independent)}$$

$$\therefore \quad f_{nR}(t) = \frac{-2\sqrt{2}\, A_o}{n\pi\omega_{nR}} \int_0^L \sin\left[\omega_{nR}(t-\tau)\right] d\tau.$$

Substituting for ω_{nR} in the above equation gives:

$$f_{nR}(t) = \frac{-8\sqrt{2}\ A_o L^2}{n^3\pi^3 a^2}\ [1-\cos(n\pi at/2L)] \ . \qquad (2.28)$$

where: n = 1, 3, 5, 7 ---- .

Recalling the definition of the constant "a",

$$a^2 = AE/\rho$$

$$\therefore \quad a^2/L^2 = AE/\rho L^2 \ .$$

Substituting for a^2/L^2 into eq. (2.28) gives:

$$f_{nR}(t) = \frac{-8\sqrt{2}\ A_o \rho L^2}{n^3\pi^3 AE}\ [1-\cos(\frac{n\pi t}{2}\sqrt{AE/\rho L^2})] \ , \text{ and} \qquad (2.29)$$

$$\omega_{nR} = \frac{n\pi a}{2L} = \frac{n\pi}{2}\sqrt{AE/\rho L^2} \ . \qquad (2.30)$$

where: n = odd integer.

Furthermore, from the general form of the solution,

$$u_R(x,t) = \sum_{n=1}^{\infty} U_{nR}(x)\ f_{nR}(t) \ .$$

Hence, the total solution becomes:

$$u_R(x,t) = \frac{-16\ A_o \rho L^2}{\pi^3 AE} \sum_{n=1,3,5,----} 1/n^3 \cdot [1-\cos(\frac{n\pi t}{2}\sqrt{AE/\rho L^2})] \sin(\frac{n\pi x}{2L}) \ . \qquad (2.31)$$

Note that, to find the base stresses it is the relative displacement which is of primary interest and not the absolute displacement. Moreover, it is easier to work with the relative mass deflections in the lumped parameter models. In as

much as the rigid body part of the solution is not considered in the case of continuous systems and the lumped parameter models, for comparisons of end deflections and strain-energy, eq. (2.31) represents the total displacement solution for the continuous system to a constant base acceleration excitation.

The relative end deflections and base stresses are found in order to verify the validity of the method employed as these responses have been established in a previous paper.[2] This will also keep the study in consistent comparison with the previous work.

The relative end deflection of the rod is given by:

$$u_R(L,t) = \frac{-16\ A_o\rho L^2}{\pi^3 AE} \sum_{n=1,3,5,----} 1/n^3 . \sin(n\pi/2)\,[1-\cos(\frac{n\pi t}{2}\sqrt{AE/\rho L^2})]$$

and its maximum value is found by summing up the series:

$$u_R(L,t)_{max} = \frac{-32A_o\rho L^2}{\pi^3 AE} \sum_{n=1,3,5,----} 1/n^3 . \sin(n\pi/2) \quad . \qquad (2.32)$$

Obviously this maximum value is first reached at $t = 2\sqrt{\rho L^2/AE}$. Stress in the bar is found from the relation:

$$\sigma(x,t) = E(\frac{\partial u_R}{\partial x}) \ , \text{ or}$$

$$\sigma(x,t) = \frac{-8A_o\rho L}{\pi^2 A} \sum_{n=1,3,5,----} 1/n^2 . \cos(n\pi x/2L)\ [1-\cos(\frac{n\pi t}{2}\sqrt{AE/\rho L^2})] \ .$$

This is maximum at x = 0, i.e., at the base. Thus, the maximum stress in the bar occurs at the base and is given by:

$$\sigma(0,t) = \frac{-8A_o\rho L}{\pi^2 A} \sum_{n=1,3,5,----} 1/n^2 . \ [1-\cos(\frac{n\pi t}{2}\sqrt{AE/\rho L^2})] \ .$$

Again, this base stress first reaches its peak value at

$t = 2\sqrt{\rho L^2/AE}$.

The maximum base stress can be obtained from:

$$\sigma(0,t) = \frac{-16A_o\rho L}{\pi^2 A} \sum_{n=1,3,5,----} 1/n^2$$

$$= \frac{-2A_o\rho L}{A} . \qquad (2.33)$$

C.2 Half Sine Pulse Type of Base Acceleration Excitation

The half sine pulse type of base acceleration has been chosen to demonstrate the effect of time varying excitations. The period of the half sine pulse has been examined for four different cases,

(i) Period of the half sine pulse made equal to half of the fundamental period of the system.

(ii) The pulse period made 10% less than the fundamental period.

(iii) The pulse period made 10% greater than the fundamental period and

(iv) The pulse period made 50% greater than the fundamental period.

The first and the last cases exhibit the effect of having a fast and a slow system, respectively, while the other two cases exhibit the effect of the forced excitation frequency near the fundamental frequency of the system.

A half sine pulse type of base acceleration is applied at the left end of the rod and the right end is free.

Figure 4 shows a half sine pulse with the duration time of πt_1. The equation of the pulse is given by $A_o \sin(t/t_1)$, where A_o is the peak amplitude of the pulse.

The governing equation used previously is directly applicable as only the forcing function is being changed, that is:

$$\ddot{f}_{nR}(t) + \omega_{nR}^2 . f_{nR}(t) = - 2\sqrt{2}\, \ddot{u}_B/n\pi \ .$$

$$U_{nR}(x) = \sqrt{2}\, \sin(n\pi x/2L) \ , \text{ and}$$

$$\omega_{nR} = n\pi a/2L \ , \ n = \text{odd integer.}$$

For a half sine pulse, the base acceleration function now becomes:

$$\ddot{u}_B = A_o \sin(t/t_1) \ .$$

$$\therefore \quad \ddot{f}_{nR}(t) + \omega_{nR}^2 . f_{nR}(t) = \frac{-2\sqrt{2}A_o \sin(t/t_1)}{n\pi} \ . \qquad (2.34)$$

Again Duhamel's integral solution can be used to obtain the solution to $f_{nR}(t)$.

The solution of the problem with the half sine pulse type of excitation is obtained in two parts; one is valid for time t less than πt_1 (the total duration of the pulse) and the other, valid for time t greater than the pulse time, πt_1. Both these solutions are obtained by the Duhamel's integral, care being taken with the limits of the integral.

For $o<t\leqslant\pi t_1$ the solution is given by:

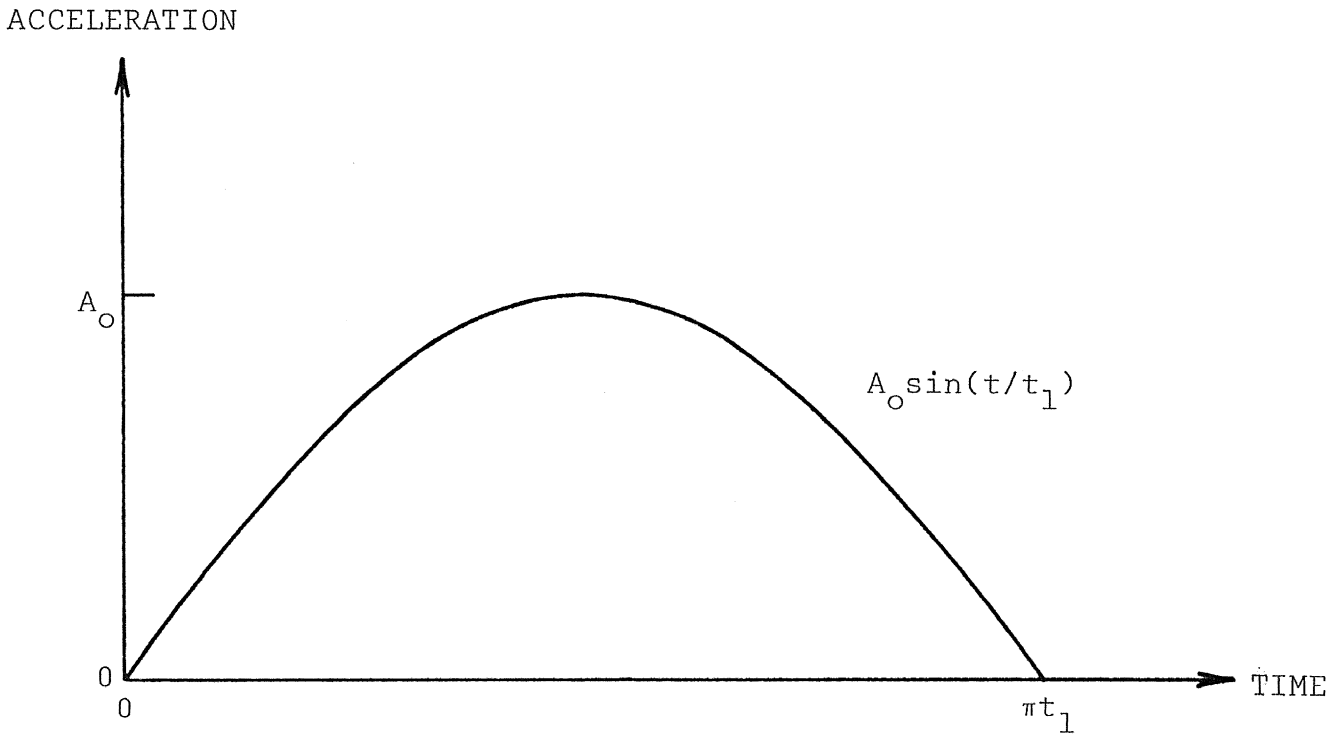

Fig. 4 Half Sine Pulse Applied as Base Acceleration

$$f_{nR}(t) = \int_0^t \frac{\sin\ \omega_{nR}(t-\tau)}{\omega_{nR}} F(\tau)\ d\tau$$

$$= \int_0^t \frac{\sin\ \omega_{nR}(t-\tau)}{\omega_{nR}} \cdot \frac{-2\sqrt{2}A_o \sin(\tau/t_1)}{n\pi}\ d\tau\ , \text{ or}$$

$$f_{nR}(t) = \frac{-\sqrt{2}A_o}{\omega_{nR} n\pi} \int_0^t [\cos(\omega_{nR}t-\omega_{nR}\tau-\frac{\tau}{t_1})-\cos(\omega_{nR}t-\omega_{nR}\tau+\frac{\tau}{t_1})]\cdot d\tau$$

$$= \frac{-\sqrt{2}A_o}{\omega_{nR} n\pi} \left[\frac{\sin(\omega_{nR}t-\omega_{nR}\tau-\tau/t_1)}{-(\omega_{nR}+1/t_1)} - \frac{\sin(\omega_{nR}t-\omega_{nR}\tau+\tau/t_1)}{-(\omega_{nR}-1/t_1)} \right]_0^t$$

$$= \frac{-2\sqrt{2}A_o}{\omega_{nR} n\pi} [\omega_{nR}\sin(t/t_1)-1/t_1\sin(\omega_{nR}t)] \Big/ (\omega_{nR}^2-1/t_1^2)\ .$$

As already found for fixed-free ends:

$$\omega_{nR} = n\pi a/2L\ , \text{ and}$$

$$a = \sqrt{AE/\rho}\ .$$

$$\therefore \quad \omega_{nR} = \frac{n\pi}{2L}\sqrt{AE/\rho}\ . \qquad (2.35)$$

Therefore, for $o<t\leq\pi t_1$:

$$f_{nR}(t) = \frac{-4\sqrt{2}A_o}{n^2\pi^2}\sqrt{\frac{\rho L^2}{AE}} \left[\frac{n\pi}{2L}\sqrt{\frac{AE}{\rho}}\ \sin(t/t_1)-1/t_1\sin(\frac{n\pi}{2L}\sqrt{\frac{AE}{\rho}}\ t) \right]$$

$$\Big/ \left[(\frac{n\pi}{2L}\sqrt{AE/\rho})^2 - 1/t_1^2 \right]\ . \qquad (2.36)$$

Since $u_R(x,t) = \sum_{n=1,3,5,----} U_{nR}(x)\ f_{nR}(t)$, it follows:

$$u_R(x,t) = \frac{-8A_o}{\pi^2}\sqrt{\frac{\rho L^2}{AE}} \sum_{n=1,3,5,----} 1/n^2 \cdot \frac{\left[\frac{n\pi}{2L}\sqrt{\frac{AE}{\rho}}\sin(t/t_1) - \frac{1}{t_1}\sin(\frac{n\pi}{2L}\sqrt{\frac{AE}{\rho}}\,t)\right]}{\left[(\frac{n\pi}{2L}\sqrt{AE/\rho})^2 - 1/t_1^2\right]}$$

$$\cdot \sin(n\pi x/2L). \qquad (2.37)$$

The relative displacement $u_R(x,t)$ for $t \geq \pi t_1$ is obtained by again using the Duhamel's integral. Using eq. (2.34) for all $t \geq \pi t_1$ gives:

$$f_{nR}(t) = \int_0^{\pi t_1} \frac{\sin\,\omega_{nR}(t-\tau)}{\omega_{nR}} F_1(\tau)\,d\tau + \int_{\pi t_1}^{t} \frac{\sin\,\omega_{nR}(t-\tau)}{\omega_{nR}} F_2(\tau)\,d\tau$$

where $F_1(\tau)$ is the external force, as a function of τ, acting during the period $0 < t \leq \pi t_1$ and $F_2(\tau)$ is the external force acting during $t \geq \pi t_1$. Note that $F_2(\tau) = 0$,

$$\therefore \quad f_{nR}(t) = \int_0^{\pi t_1} \frac{\sin\,\omega_{nR}(t-\tau)}{\omega_{nR}} F_1(\tau)\,d\tau \text{ , or}$$

$$f_{nR}(t) = \int_0^{\pi t_1} \frac{\sin\,\omega_{nR}(t-\tau)}{\omega_{nR}} \cdot \frac{-2\sqrt{2}A_o \sin(\tau/t_1)}{n\pi}\,d\tau$$

$$= \frac{-\sqrt{2}A_o}{\omega_{nR} n\pi} \int_0^{\pi t_1} \left[\cos(\omega_{nR}t - \omega_{nR}\tau - \frac{\tau}{t_1}) - \cos(\omega_{nR}t - \omega_{nR}\tau + \frac{\tau}{t_1})\right] d\tau ,$$

or

$$f_{nR}(t) = \frac{2\sqrt{2}A_o}{\omega_{nR} n\pi t_1}\left[\frac{\sin\,\omega_{nR}(t-\pi t_1) + \sin(\omega_{nR}t)}{(\omega_{nR}^2 - 1/t_1^2)}\right]. \qquad (2.38)$$

Since, $u_R(x,t) = \sum_{n=1,3,5,----} U_{nR}(x)\, f_{nR}(t)$, and

$U_{nR}(x) = \sqrt{2}\,\sin(\frac{n\pi x}{2L})$, it follows that for all time $t \geq \pi t_1$:

$$u_R(x,t) = \frac{8A_o}{\pi^2 t_1}\sqrt{\frac{\rho L^2}{AE}}\sum_{n=1,3,5,----} 1/n^2 \cdot \frac{\left[\sin\{\frac{n\pi}{2L}\sqrt{\frac{AE}{\rho}}(t-\pi t_1)\}+\sin(\frac{n\pi}{2L}\sqrt{\frac{AE}{\rho}}\ t)\right]}{\left[(\frac{n\pi}{2L}\sqrt{AE/\rho})^2-1/t_1^{\,2}\right]}$$

$$\cdot \sin(n\pi x/2L) \ . \qquad (2.39)$$

The period of the half sine pulse is given by $2\pi t_1$ and is varied for four different cases as explained below:

$$2\pi t_1 = k \cdot 2\pi/\omega_{1R}$$

where k is a constant and is made equal to 0.5 in the first case, 0.90 in the second, 1.10 in the third and 1.50 in the last case to study all the four cases of the duration of the pulse time. Therefore, for k = 0.5

$$2\pi t_1 = 0.5\ 2\pi/\omega_{1R} \ , \text{ or}$$

$$t_1 = 0.5/\omega_{1R}$$

is obtained. Similarly other values of t_1 for k = 0.9, 1.10 and 1.50 are obtained and are shown below:

k = 0.90	k = 1.10	k = 1.50
$t_1 = 0.9/\omega_{1R}$	$t_1 = 1.10/\omega_{1R}$	$t_1 = 1.50/\omega_{1R}$

The relative displacement function $u_R(x,t)$ can be evaluated for all the four cases of the pulse duration by using eqs. (2.37) and (2.39) for $0 < t \leq \pi t_1$ and $t \geq \pi t_1$, respectively.

D. Strain Energy for Principal Modes

The objective of this report is to compare the behavior of the lumped parameter models using strain energy as the

basis for this accuracy comparison. Strain energy of the continuum, therefore, needs to be established for each principal mode. The maximum strain energy determined for each lumped parameter model in a principal mode is then compared to the established exact (continuous) solution to determine how well the principal modes are described by these models.

The derivation of an expression which evaluates the strain energy of the continuum as a function of the mode number, ν, is given in this section. Referring to fig. 1, the potential strain energy for the element dx is given by:

$$dU_c = \frac{1}{2} P \left(\frac{\partial u}{\partial x}\right) dx \qquad (2.40)$$

where P is the force acting on the element dx and assumed to be constant over the length dx. From the relation,

Force = stress x resisting area

it follows that:

$$P = E\left(\frac{\partial u}{\partial x}\right) A \ .$$

Therefore, for the element dx:

$$dU_c = \frac{1}{2} AE \left(\frac{\partial u}{\partial x}\right)^2 dx \qquad (2.41)$$

is obtained.

Strain energy, over the entire length of the bar, is obtained by integrating eq. (2.41) from 0 to L. The total strain energy of the system is, therefore:

$$U_c = \int_0^L 1/2 \ AE\left(\frac{\partial u}{\partial x}\right)^2 dx \ , \text{ or}$$

$$U_c = 1/2 \ AE \int_0^L \left(\frac{\partial u}{\partial x}\right)^2 dx \ . \qquad (2.42)$$

(since for the system under consideration AE is constant).

Equation (2.42) gives the strain energy of a uniform thin bar and can be used to determine the strain energy of the continuous system with fixed-fixed and fixed-free end conditions. In fact, eq. (2.42) can be used for any type of boundary conditions.

Fixed-Fixed Boundary Conditions

The mode shapes are given by:

$$U_\nu(x) = D_\nu \sin(\nu\pi x/L) \ .$$

The normalization constant, D_ν, is obtained by normalizing the first orthogonality relation to the total mass of the bar, i.e.,

$$\int_0^L \rho \, U_\nu^2(x) \, dx = \rho L \qquad (2.43)$$

where ρ is the mass per unit length of the bar, which is constant for the system under consideration.

Substituting for $U_\nu(x)$ in eq. (2.43),

$$D_\nu^2 = \frac{L}{\int_0^L \sin^2(\nu\pi x/L) \, dx}$$

is obtained.

$$\therefore \quad D_\nu = \sqrt{2} \ , \text{ and}$$

$$U_\nu(x) = \sqrt{2} \sin(\nu\pi x/L) \ . \qquad (2.44)$$

For a particular νth mode, the maximum displacement as a function of position 'x' is given by:

$$u(x,t)_{max} = U_\nu(x)$$

$$= \sqrt{2} \sin(\frac{\nu\pi x}{L}) \ .$$

Maximum strain energy for this νth mode is obtained from eq. (2.42) and is given by:

$$U_{c_{max}} = \frac{1}{2}AE\int_0^L \left(\frac{\partial U_\nu(x)}{\partial x}\right)^2 . dx$$

$$= \frac{1}{2}AE\int_0^L 2\left(\frac{\nu\pi}{L}\right)^2 \cos^2\left(\frac{\nu\pi x}{L}\right). dx$$

$$= \frac{1}{2}\frac{AE}{L}(\nu\pi)^2 . \qquad (2.45)$$

Fixed-Free Boundary Conditions

The mode shapes for these end conditions are given by:

$$U_\nu(x) = D_\nu \sin[(2\nu-1)\pi x/2L] .$$

The normalization constant, D_ν, is found in the same manner as for fixed-fixed end conditions explained earlier. From the first normalization relation:

$$\int_0^L U_\nu^2(x)\, dx = L .$$

$$\therefore \quad D_\nu^2 = \frac{L}{\int_0^L \sin^2[(2\nu-1)\pi x/2L]\cdot dx} , \text{ or}$$

$$D_\nu = \sqrt{2} , \text{ and}$$

$$U_\nu(x) = \sqrt{2}\sin[(2\nu-1)\pi x/2L] . \qquad (2.46)$$

Using eq. (2.42), maximum strain energy for the νth mode is given by:

$$U_{c_{max}} = \frac{1}{2}AE\int_0^L 2\{(2\nu-1)\pi/2L\}^2\cos^2[(2\nu-1)\pi x/2L].dx$$

$$= \frac{1}{8}\frac{AE}{L}[(2\nu-1)\pi]^2 . \qquad (2.47)$$

E. Strain Energy for Forced Excitation

To study the behavior of the lumped parameter models under transient conditions, using strain energy as the basis of comparison, it is essential to evaluate an expression for the strain energy of the continuous systems under similar transient conditions. Equation (2.42) is used for the evaluation of strain energy for both the constant base acceleration type of excitation and the half sine pulse type of excitation.

Constant Base Acceleration Excitation

Differentiation of eq. (2.31) yields:

$$\frac{\partial u_R}{\partial x} = \frac{-8A_o\rho L}{\pi^2 AE}\sum_{n=1,3,5,----} 1/n^2\cdot\cos(n\pi x/2L)\left[1-\cos\left(\frac{n\pi t}{2}\sqrt{\frac{AE}{\rho L^2}}\right)\right] .$$

Strain energy of the system with a constant base acceleration, A_o, is given by:

$$U_c = \frac{1}{2}AE\int_0^L \left(\frac{\partial u_R}{\partial x}\right)^2 dx \text{ , or}$$

$$U_c = \frac{32AE}{\pi^4}\left[\frac{A_o\rho L}{AE}\right]^2\int_0^L \left[\sum_{n=1,3,5,----} 1/n^2\cdot\cos(n\pi x/2L)\left\{1-\cos\left(\frac{n\pi t}{2}\sqrt{\frac{AE}{\rho L^2}}\right)\right\}\right]^2 . dx$$

$$= \frac{32AE}{\pi^4}\left[\frac{A_o\rho L}{AE}\right]^2\int_0^L \left[\sum_{n=1,3,5,----} 1/n^2\cdot\cos(n\pi x/2L)\left\{1-\cos\left(\frac{n\pi t}{2}\sqrt{\frac{AE}{\rho L^2}}\right)\right\}\right] \cdot \left[\sum_{m=1,3,5,----} 1/m^2\cdot\cos\left(\frac{m\pi x}{2L}\right)\left\{1-\cos\left(\frac{m\pi t}{2}\sqrt{\frac{AE}{\rho L^2}}\right)\right\}\right] dx .$$

From the orthogonality and normalization relations of the system in question:

$$\int_0^L U'_{nR}(x)\, U'_{mR}(x).dx = 0 \text{ , } m\neq n$$

$$= \int_0^L U'^2_{nR}.dx, \text{ } m=n .$$

$$\therefore U_c = \frac{32AE}{\pi^4}\left(\frac{A_o \rho L}{AE}\right)^2 \int_0^L \left[\sum_{n=1,3,5,----} 1/n^4 \cdot \cos^2(n\pi x/2L)\{1-\cos(\frac{n\pi t}{2}\sqrt{\frac{AE}{\rho L^2}})\}^2\right] \cdot dx$$

$$= \frac{16AEL}{\pi^4}\left(\frac{A_o \rho L}{AE}\right)^2 \sum_{n=1,3,5,----} 1/n^4 \cdot [1-\cos(\frac{n\pi t}{2}\sqrt{\frac{AE}{\rho L^2}})]^2 \quad . \tag{2.48}$$

Obviously this is maximum at $t = 2\sqrt{\frac{\rho L^2}{AE}}$. The maximum system strain energy is, therefore, given by:

$$U_{c_{max}} = \frac{64 A_o^2 \rho^2 L^3}{\pi^4 AE} \sum_{n=1,3,5,----} 1/n^4$$

$$= 2A_o^2 \rho^2 L^3/3AE \quad . \tag{2.49}$$

Half Sine Pulse Base Acceleration Excitation

Strain energy for half sine pulse base acceleration type of excitation is obtained in two parts, one for $0<t\leqslant \pi t_1$ and the other for $t\geqslant \pi t_1$, by using applicable displacement functions in eq. (2.42).

For $0<t\leqslant \pi t_1$, using eq. (2.37), strain energy, U_c, is given by:

$$U_c = \frac{1}{2}AE \int_0^L \left[\frac{-4A_o}{\pi L}\sqrt{\frac{\rho L^2}{AE}} \sum_{n=1,3,5,----} 1/n \cdot \frac{\left[\frac{n\pi}{2L}\sqrt{\frac{AE}{\rho}}\sin(t/t_1) - 1/t_1 \sin(\frac{n\pi}{2L}\sqrt{\frac{AE}{\rho}}\, t)\right]}{\{(\frac{n\pi}{2L}\sqrt{\frac{AE}{\rho}})^2 - 1/t_1^2\}} \cdot \cos(\frac{n\pi x}{2L})\right]^2 \cdot dx$$

$$= \frac{8A_o^2 \rho}{\pi^2} \sum_{n=1,3,5,----} 1/n^2 \cdot \frac{\left[\frac{n\pi}{2L}\sqrt{\frac{AE}{\rho}}\sin(t/t_1) - 1/t_1 \sin(\frac{n\pi}{2L}\sqrt{\frac{AE}{\rho}}\, t)\right]^2}{\{(\frac{n\pi}{2L}\sqrt{\frac{AE}{\rho}})^2 - 1/t_1^2\}^2}$$

$$\cdot \int_0^L \cos^2(n\pi x/2L) \cdot dx \quad , \text{ or}$$

$$U_c = \frac{4A_o \rho L}{\pi^2} \sum_{n=1,3,5,----} 1/n^2 \frac{\left[\frac{n\pi}{2L}\sqrt{\frac{AE}{\rho}}\sin(t/t_1) - 1/t_1 \sin(\frac{n\pi}{2L}\sqrt{\frac{AE}{\rho}}\, t)\right]^2}{\{(\frac{n\pi}{2L}\sqrt{\frac{AE}{\rho}})^2 - 1/t_1^2\}^2} \quad . \tag{2.50}$$

The strain energy expression is also needed for $t \geqslant \pi t_1$ since maximum strain energy may occur after the pulse time. To establish an expression for the strain energy for all $t \geqslant \pi t_1$, $u_R(x,t)$ for $t \geqslant \pi t_1$ is used from eq. (2.39):

$$u_R(x,t) = \frac{8A_o}{\pi^2 t_1}\sqrt{\frac{\rho L^2}{AE}} \sum_{n=1,3,5,----} 1/n^2 \frac{\left[\sin\frac{n\pi}{2L}\sqrt{\frac{AE}{\rho}}(t-\pi t_1) + \sin(\frac{n\pi t}{2L}\sqrt{\frac{AE}{\rho}})\right]}{\{(\frac{n\pi}{2L}\sqrt{\frac{AE}{\rho}})^2 - 1/t_1^2\}} \cdot \sin(\frac{n\pi x}{2L}) \quad .$$

Substituting for $\frac{\partial u_R}{\partial x}$ in eq. (2.42), strain energy of the system can be evaluated as:

$$U_c = \frac{1}{2}AE\int_0^L \left[\frac{4A_o}{\pi t_1 L}\sqrt{\frac{\rho L^2}{AE}} \sum_{n=1,3,5,----} 1/n \frac{\left[\sin\{\frac{n\pi}{2L}\sqrt{\frac{AE}{\rho}}(t-\pi t_1)\} + \sin(\frac{n\pi t}{2L}\sqrt{\frac{AE}{\rho}})\right]}{\{(\frac{n\pi}{2L}\sqrt{\frac{AE}{\rho}})^2 - 1/t_1^2\}} \cdot \cos(\frac{n\pi x}{2L})\right]^2 dx$$

$$= \frac{4A_o \rho L}{\pi^2 t_1^2} \sum_{n=1,3,5,----} 1/n^2 \frac{\left[\{\sin\frac{n\pi}{2L}\sqrt{\frac{AE}{\rho}}(t-\pi t_1)\} + \sin(\frac{n\pi t}{2L}\sqrt{\frac{AE}{\rho}})\right]^2}{\left[(\frac{n\pi}{2L}\sqrt{\frac{AE}{\rho}})^2 - 1/t_1^2\right]^2} \quad . \tag{2.51}$$

The strain energy for all four cases of half sine pulse, for $0 < t \leqslant \pi t_1$ and for $t \geqslant \pi t_1$ can be obtained from eqs. (2.50) and (2.51), respectively. Maximum system strain energy can be computed by evaluating numerically eqs. (2.50) and (2.51) for various values of time 't'. This will be discussed in

chapter IV where the comparison between model and continuum is presented.

CHAPTER III

LUMPED PARAMETER MODELS

A. Model Definitions

Three lumped parameter models commonly used to describe one-dimensional systems are shown in fig. 5. These models each approximate the mass and stiffness of one increment of a uniform continuous system composed of N segments. Model (a), which was first used by Rayleigh, has the total mass of each of the N increments, into which the bar has been segmented, divided into two equal masses concentrated at each end of a spring which represents the stiffness of the increment. The second model has been attributed in the literature to Lagrange but has been investigated to some extent by Duncan[1] and is sometimes referred to as Duncan's model. This model has the mass of the increment concentrated at the center with equal springs on each side. The third one, model (c), which has been used to a large extent in practice, has the mass concentrated at one end of a spring.

A new method, under the consistent mass matrix technique, developed by John Archer[3], has been applied to one-dimensional systems by A. V. Krishna Murty[4]. This new method evaluates the equivalent inertia forces of the elements at the discrete displacement points instead of lumping the masses in the conventional models discussed above. The method also requires selection of a suitable displacement distribution function over each element and as in Rayleigh-Ritz method, the closer the displacement function to the exact mode shape, the better

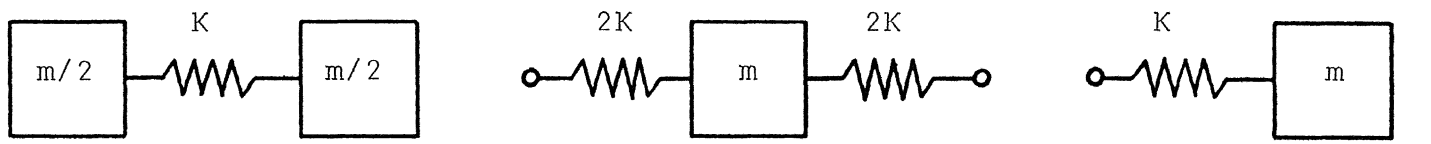

MODEL (a) MODEL (b) MODEL (c)

$K = AE/l$, $l = L/N$

Fig. 5 Lumped Parameter Models

the result. The frequency roots found by this method have been shown to be slightly more accurate than those found by using the models.

In this report only the conventional models will be studied using the strain energy approach. However, the consistent mass matrix also needs to be studied on the basis of system strain energy.

B. Homogeneous Solutions

Various methods are available for establishing the principal mode shapes for the lumped parameter models, e.g., the modal matrix technique and the difference equation approach. The latter method which is particularly useful for repeated sections has been used for models (a) and (c). For model (b), this approach gives displacements at the points between adjacent springs of the two connecting segments and not at the mass points as desired. Mass point deflections for model (b), therefore, have been obtained in conjunction with the use of the IBM-360-50 computer utilizing a standard eigenvalue subroutine from the system library.

Mode shapes for the models under consideration are derived as described in the following subsection.

Model (a) with Fixed-Fixed Ends

The difference equation approach is used to establish the mode shapes (see Appendix A) for this case:

$$X_{\bar{N}} = E_{\nu}\cos(\beta\bar{N}) + F_{\nu}\sin(\beta\bar{N}) \qquad (3.1)$$

where: $\bar{N} = 0,1,2,\ldots\ldots, N$ and refers to the mass point location in the system

ν = mode number = $1,2,3,4,\ldots\ldots$, up to the number of masses.

The boundary conditions impose following restrictions on the spatial functions:

$$X_0 = E_\nu = 0 \quad \text{and} \quad X_N = F_\nu \sin(\beta N) = 0$$

which gives:

$$X_{\bar{N}} = F_\nu \sin(\bar{N}\nu\pi/N) \tag{3.2}$$

where: F_ν is a normalization constant.

Model (a) with Fixed-Free Ends

The fixed end condition gives:

$$X_0 = E_\nu = 0 \ .$$

$$\therefore \quad X_{\bar{N}} = F_\nu \sin(\beta\bar{N}) \ .$$

In this model representation with fixed-free ends, the Nth mass (i.e., mass at the free end) is not equal to other masses in the system and in order to apply the difference equation solution, which is applicable to repeated sections only, the motion of the Nth mass is examined and a condition for the rest of the system is evaluated at this mass as shown below.

Considering the equilibrium of the Nth mass:

$$\frac{m}{2} \ddot{x}_N = -K(x_N - x_{N-1}) \ .$$

Form of the solution is given by:

$$x_{\bar{N}} = X_{\bar{N}} \, e^{i\omega t} \ .$$

Substituting this form of solution in the above equation,

$$\frac{-\omega^2 m}{2} X_N = -K(X_N - X_{N-1})$$

is obtained.

$$\therefore \quad X_{N-1} = \left(1 - \frac{m\omega^2}{2K}\right) X_N \ .$$

Substituting for X_{N-1} and X_N, the above equation becomes:

$$\sin\{\beta(N-1)\} = \left(1 - \frac{m\omega^2}{2K}\right) \sin(\beta N) \ .$$

Noting that, $\left(1 - \frac{m\omega^2}{2K}\right) = \cos(\beta)$ then,

$$\sin\{\beta(N-1)\} = \cos(\beta) \sin(\beta N)$$

which gives:

$$\sin(\beta) \cos(\beta N) = 0 \ .$$

Therefore, either $\sin(\beta) = 0$ or $\cos(\beta N) = 0$.

$\sin(\beta) = 0$ gives the trivial solution,

$X_{\bar{N}} = 0$, i.e., no vibrations.

For vibrations to occur $\cos(\beta N) = 0$, or

$$\beta = (2\nu - 1)\pi/2N \ .$$

$$\therefore \quad X_{\bar{N}} = F_\nu \sin[(2\nu-1)\pi\bar{N}/2N] \ . \qquad (3.3)$$

Model (b) with Fixed-Fixed Ends

The difference equation approach is not applicable in this case since it gives displacements at the points between adjacent springs of the two adjacent segments and not at the mass points of the model as desired. These displacements are given by eqs. (3.2) and (3.3) for fixed-fixed and fixed-free

ends, respectively. To determine the mass displacements standard eigenvalue techniques are used. The differential equations of motion in matrix form are first reduced to a desirable form in order to facilitate finding of eigenvalues and eigenvectors of the system. The differential equations of motion in matrix notation are given by:

$$\lceil m \rfloor \{\ddot{x}\} + [K]\{x\} = \{0\} \ . \qquad (3.4)$$

It should be noted here that the mass matrix [m] is always a diagonal matrix for model (b) and each diagonal element, m_{ii}, is equal to m (the mass of each segment). The general form of the stiffness matrix [K] for model (b) with fixed-fixed ends is given by:

$$[K] = \begin{bmatrix} 3K & -K & & & \\ -K & 2K & & 0 & \\ & \ddots & \ddots & & \\ & & & 2K & -K \\ & 0 & & -K & 3K \end{bmatrix} \quad N \times N \text{ MATRIX}$$

where: $K = AE/l$ and $l = L/N$.

Premultiplication of eq. (3.4) by $\lceil m \rfloor^{-1}$ yields:

$$\{\ddot{x}\} + \lceil m \rfloor^{-1}[K]\{x\} = \{0\} \ .$$

It may be noted that matrix [K] is a symmetric matrix and $\lceil m \rfloor^{-1}[K]$ is also a symmetric matrix in this particular case, since $\lceil m \rfloor^{-1}$ is equal to $\frac{1}{m}[I]$, where [I] is an identity matrix.

A standard eigenvalue subroutine from the IBM-360-50 computer library was employed to find the eigenvalues and eigenvectors of $\lceil m \rfloor^{-1}[K]$. The square root of the eigenvalues

gives the natural frequencies of the system. The eigenvectors obtained are normalized just as in the continuous system, by using the normalized equation in matrix notation, i.e.,

$$D_\nu^2 \{x\}^T [m] \{x\} = m N \quad , \text{ and}$$

$$\{U_\nu(x)\} = D_\nu \{x\} \quad , \text{ or}$$

$$= \frac{(mN)^{\frac{1}{2}} \{x\}}{(\{x\}^T [m] \{x\})^{\frac{1}{2}}} \ .$$

Model (b) with Fixed-Free Ends

The procedure for finding the eigenvalues and the eigenvectors, of model (b) with fixed-free ends, is exactly the same as that used for model (b) with fixed-fixed ends, except for the change in the stiffness matrix [K]. The stiffness matrix [K], in general form, for model (b) with fixed-free ends is of the form:

$$[K] = \begin{bmatrix} 3K & -K & & \\ -K & 2K & & 0 \\ & & \ddots & \\ & 0 & & 2K \ -K \\ & & & -K \ \ K \end{bmatrix} N \times N \text{ MATRIX}$$

where: $K = AE/l$ and $l = L/N$.

Model (c) with Fixed-Fixed Ends

Models (a) and (c) are exactly alike for fixed-fixed boundary conditions. Thus the solutions for model (a) with fixed-fixed ends, established earlier, can also be used for model (c) with fixed-fixed ends.

Model (c) with Fixed-Free Ends

The fixed boundary condition gives:

$$X_0 = E_\nu = 0.$$

The free boundary condition gives:

$$\cos\beta(N+\tfrac{1}{2}) = 0, \text{ or}$$

$$\beta = \frac{(2\nu-1)\pi}{(2N+1)}$$

$$\therefore \quad X_{\bar{N}} = F_\nu \sin\left[(2\nu-1)\pi\bar{N}/(2N+1)\right] \qquad (3.5)$$

C. Forced Excitation Solutions

For means of comparisons, the two types of excitation used for the continuous systems will be employed for the lumped parameter models. These are:

(i) constant base acceleration

(ii) half sine pulse base acceleration.

In each case a analogue system of the model relating to the continuous bar with base acceleration, $\ddot{u}_B(t)$, is obtained. This new system gives the mass point deflections relative to the base, the base stresses and the strain energy to be compared with the corresponding results obtained for the continuum.

Relative Coordinate Formulation

The formulation of the analogue systems can be shown by an example with the number of segments in the model being three. Figure 6 shows model (a) with 3 segments and with a base displacement or displacement of mass m_1, as u_B and base acceleration as $\ddot{u}_B$ which are general time-varying functions.

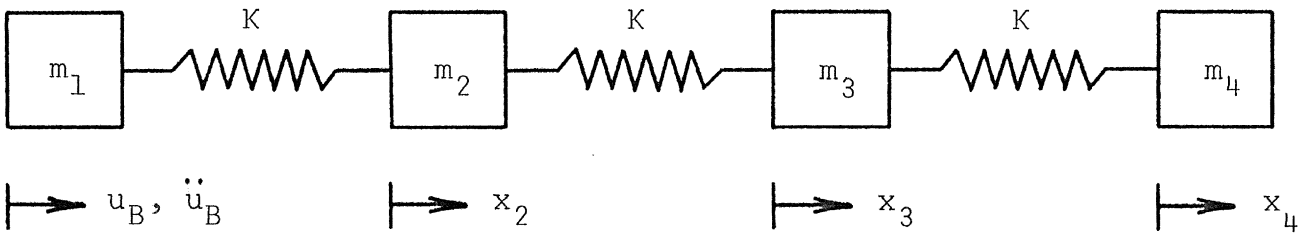

Fig. 6 Model (a) with N=3 and Base Acceleration $\ddot{u}_B(t)$

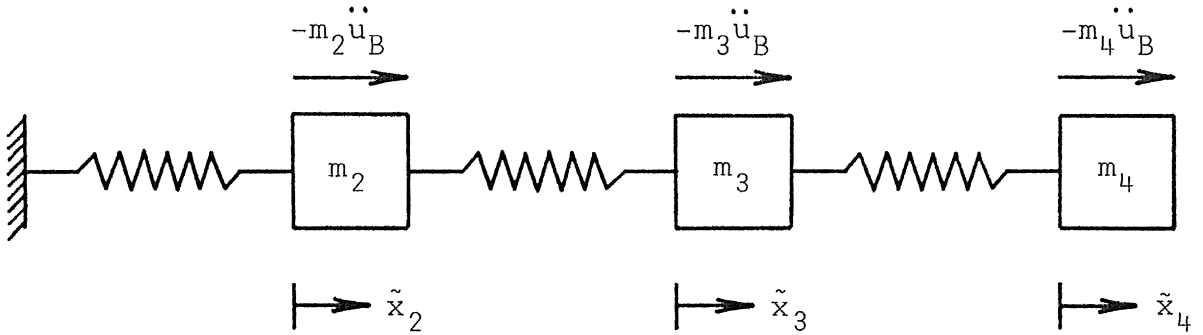

Fig. 6a Relative Coordinate Formulation

The absolute displacements of masses m_2, m_3 and m_4 are given by x_2, x_3 and x_4, respectively, in fig. 6. Each spring in figs. 6 and 6a has the same stiffness $K = AE/l = \frac{AE}{L/N}$, where L is the total length of the bar and N is the number of segments used in the model representation.

Figure 6a shows a system with a fixed base and displacements $\tilde{x}_2$, $\tilde{x}_3$ and $\tilde{x}_4$ of masses m_2, m_3 and m_4, respectively, which are displacements measured relative to the base. Therefore, in this new system the base is shown to be fixed. It will now be shown that the system with its base fixed and each mass having (fig. 6a) an external force, proportional to its own mass, has similar differential equations as those of the system with a base acceleration, $\ddot{u}_B$ (fig. 6).

Referring to fig. 6, the differential equations of motion for m_2, m_3 and m_4 are:

$$m_2\ddot{x}_2+2Kx_2-Kx_3-Ku_B = 0 \qquad (3.6)$$

$$m_3\ddot{x}_3-Kx_2+2Kx_3-Kx_4 = 0 \qquad (3.7)$$

$$m_4\ddot{x}_4 \quad -Kx_3+Kx_4 = 0 \ . \qquad (3.8)$$

The displacements, $\tilde{x}$, of the system in fig. 6a are defined as:

$$\tilde{x}_i = x_i-u_B \ , \text{ or}$$

$$x_i = \tilde{x}_i+u_B \ .$$

$$\therefore \quad \ddot{x}_i = \ddot{\tilde{x}}_i+\ddot{u}_B \ .$$

Substituting for $\tilde{x}_i$ and $\ddot{\tilde{x}}_i$ in eqs. (3.6), (3.7) and (3.8), the differential equations of motion become:

$$m_2\ddot{\tilde{x}}_2+2K\tilde{x}_2-K\tilde{x}_3 = -m_2\ddot{u}_B \qquad (3.9)$$

$$m_3\ddot{\tilde{x}}_3-K\tilde{x}_2+2K\tilde{x}_3-K\tilde{x}_4 = -m_3\ddot{u}_B \qquad (3.10)$$

$$m_4\ddot{\tilde{x}}_4-K\tilde{x}_3+K\tilde{x}_4 = -m_4\ddot{u}_B \ . \qquad (3.11)$$

It may be noted here that eqs. (3.9), (3.10) and (3.11) are similar to eqs. (3.6), (3.7) and (3.8), respectively, except for the change of coordinate system. The new system of coordinates defined by $\tilde{x}_i$ gives the relative deflections of point masses. Equations (3.9), (3.10) and (3.11) represent the system shown in fig. 6a. In matrix notation these equations can be written as:

$$[m]\{\ddot{\tilde{x}}\}+[K]\{\tilde{x}\} = -\ddot{u}_B\{m_i\} \ . \qquad (3.12)$$

These equations represent a system with the mass points having external forces proportional to the masses themselves. Thus a new system, given by eq. (3.12) and shown in fig. 6a, is formulated and is shown to be analogous to the system presented in fig. 6. This new system can be used to determine the relative end deflections given by $\tilde{x}_N$ (the displacement of the mass m_N in fig. 6a) and the base stresses per unit cross sectional area of the bar. The latter quantity is given by $\tilde{x}_2$ times the stiffness of the first spring, which depends upon the type of model under consideration. Strain energy can be evaluated by using $\tilde{x}_2$, $\tilde{x}_3$,....., $\tilde{x}_N$, directly and without considering the rigid body displacements x_2, x_3,....., x_N. It may be noted here that all solutions and conclusions derived herein for a system with external forces at the mass points,

proportional to the masses themselves, are also equally applicable to a system with base acceleration since the two systems have been shown to be analogous.

Modal Matrix for Lumped Parameter Models

The modal matrix is required to establish a solution for the relative deflection vector $\{\tilde{x}\}$ and to, thus, find the base stresses and the strain energy of the system. Computation of the relative deflections, the base stresses and the strain energy is done by using the system represented in fig. 6a for various values of N.

The differential equations of motion in matrix form for the homogeneous solution are given by:

$$\lceil m \rfloor \{\ddot{\tilde{x}}\} + [K]\{\tilde{x}\} = \{0\} \qquad (3.13)$$

where $\lceil m \rfloor$ is a diagonal mass matrix and $\{\tilde{x}\}$ is the relative displacement vector. Assuming, $\{\tilde{x}\} = \lceil m \rfloor^{-\frac{1}{2}}\{y\}$, i.e., a change of system coordinates, and substituting into eq. (3.13) gives:

$$\lceil m \rfloor \lceil m \rfloor^{-\frac{1}{2}}\{\ddot{y}\} + [K]\lceil m \rfloor^{-\frac{1}{2}}\{y\} = \{0\}$$

and premultiplying throughout by $\lceil m \rfloor^{-\frac{1}{2}}$ results in

$$\{\ddot{y}\} + \lceil m \rfloor^{-\frac{1}{2}}[K]\lceil m \rfloor^{-\frac{1}{2}}\{y\} = \{0\} .$$

It may be noted that $\lceil m \rfloor^{-\frac{1}{2}}[K]\lceil m \rfloor^{-\frac{1}{2}}$ is symmetric since $[K]$ is a symmetric matrix. Therefore, the coordinate transformation has not disturbed the symmetry of the stiffness matrix.

Using $[\bar{K}] = \lceil m \rfloor^{-\frac{1}{2}}[K]\lceil m \rfloor^{-\frac{1}{2}}$ gives:

$$\{\ddot{y}\} + [\bar{K}]\{y\} = \{0\} . \qquad (3.14)$$

$[\bar{K}]$ is now, used to determine the eigenvalues and eigenvectors. This was done using the IBM-360-50 computer utilizing a

standard eigenvalue subroutine from the system library. It can be shown that the eigenvalues of $[\bar{K}]$ are the same as those obtained using eq. (3.13). The modal matrix, formed by writing columnwise the eigenvectors of $[\bar{K}]$, is premultiplied by $[\lceil m \rfloor]^{-\frac{1}{2}}$ to obtain the modal matrix of eq. (3.13), i.e., if $[\beta]$ is the modal matrix of $[\bar{K}]$ and $[\mu]$ be that of eq. (3.13),

$$[\mu] = [\lceil m \rfloor]^{-\frac{1}{2}}[\beta] \ .$$

The normalized modal matrix $[\nu]$ of eq. (3.13) is obtained as explained below.

If $[\lceil A_i \rfloor]$ is the normalization constants matrix with normalization constants as the diagonal elements, the normalized modal matrix becomes:

$$[\nu] = [\mu][\lceil A_i \rfloor] \quad , \text{ and}$$

$$[\nu]^T[\lceil m \rfloor][\nu] = N\ m[I] \quad , \text{ or}$$

$$[\lceil A_i \rfloor][\mu]^T[\lceil m \rfloor][\mu][\lceil A_i \rfloor] = N\ m\ [I] \quad , \text{ or}$$

$$[\lceil A_i^2 \rfloor]^{-1} = \frac{[\mu]^T[\lceil m \rfloor][\mu]}{N\ m} \ . \qquad (3.15)$$

A_i can be found from eq. (3.15) and, thus, modal matrix, $[\nu]$, can be obtained from:

$$[\nu] = [\mu][\lceil A_i \rfloor] \ .$$

$[\nu]$ is, then, the required modal matrix to be used to establish the relative deflections, the base stresses and the strain energy of the lumped parameter models.

Solution by Classical Superposition of Normal Modes

Once the dynamically equivalent system is established and its modal matrix formed, the next step is to find the relative deflections of the mass points. This is done as follows.

Let, $\{\tilde{x}\} = [\nu]\{P\}$

where: $\{P\}$ are the principal coordinates.

Then, from eq. (3.12):

$$[\lceil m \rfloor][\nu]\{\ddot{P}\} + [K][\nu]\{P\} = -\ddot{u}_B\{m_i\} \ .$$

Premultiplying this by $[\nu]^T$,

$$[\nu]^T[\lceil m \rfloor][\nu]\{\ddot{P}\} + [\nu]^T[K][\nu]\{P\} = -\ddot{u}_B[\nu]^T\{m_i\} \qquad (3.16)$$

is obtained.

It may be noted that $[\nu]^T[\lceil m \rfloor][\nu]$ is normalized to $N\,m[I]$, where m is the mass of each segment and [I] is an identity matrix. Also,

$$[\nu]^T[K][\nu] = N\,m\left[\lceil \omega_i^2 \rfloor\right] \ .$$

Therefore, eq. (3.16) gives:

$$\{\ddot{P}\} + \left[\lceil \omega_i^2 \rfloor\right]\{P\} = \{F(t)\} \qquad (3.17)$$

where: $$\{F(t)\} = \frac{-\ddot{u}_B}{N\,m}[\nu]^T\{m_i\} \ .$$

Duhamel's integral can now be used to evaluate $\{P\}$ as shown below:

$$\{P\} = -\left[\lceil \omega_i \rfloor\right]^{-1}\int_0^t \left[\widetilde{\sin}\ \omega_i(t-\tau)\right]\frac{\ddot{u}_B(\tau)}{N\,m}\,[\nu]^T\{m_i\}\,d\tau \ .$$

Constant Base Acceleration Excitation

For studying the case of constant base acceleration, $\ddot{u}_B = A_o$ = constant (i.e., independent of time 't').

$$\therefore \quad \{P\} = \frac{-A_o}{Nm} \left[\omega_i\right]^{-1} \int_0^t \left[\sin \omega_i(t-\tau)\right] \left[\nu\right]^T \{m_i\}\, d\tau \ , \text{ or}$$

$$= \frac{-A_o}{Nm} \left[\omega_i\right]^{-1} \left[\frac{1-\cos \omega_i t}{\omega_i}\right] \left[\nu\right]^T \{m_i\} \ .$$

Since $\{\tilde{x}\} = [\nu]\{P\}$, it follows that:

$$\{\tilde{x}\} = \frac{-A_o}{Nm} [\nu] \left[\omega_i\right]^{-1} \left[\frac{1-\cos \omega_i t}{\omega_i}\right] \left[\nu\right]^T \{m_i\} \ . \qquad (3.18)$$

Equation (3.18) gives the relative deflections of the mass points in the system. The time-varying relative end deflection is given by $\tilde{x}_N$, the displacement of the last mass point, and its maximum value is established by selecting the maximum value of $\tilde{x}_N$ over all values of time 't'.

The relative end deflections are of importance in order to check the validity of the method by comparing the results computed herein with ones previously[2] calculated. This comparison is made in the following chapter. To verify the previous work further, base stress, in the bar, is also computed. Base stress per unit cross-sectional area of the bar is obtained by multiplying the stiffness of the first spring, from the fixed end of the system of the type shown in fig. 6a, by the relative displacement of the first mass, $\tilde{x}_2$, from the fixed end of the same system. Since $\tilde{x}_2$ is time-dependent, the base stress per unit cross-sectional area of

the bar is found for various values of time 't' and its maximum value established. Maximum base stress per unit cross-sectional area of the bar has been compared with the results obtained from the continuous analysis.

Half Sine Pulse Base Acceleration Excitation

The base acceleration, $\ddot{u}_B$, from a half sine pulse is given by:

$$\ddot{u}_B = A_o \sin(t/t_1)$$

where the duration is πt_1.

Substituting for $\ddot{u}_B$ in eq. (3.17) gives:

$$\{\ddot{P}\} + \left[\omega_i^2\right]\{P\} = \frac{-A_o \sin(t/t_1)}{N\ m}\ [\nu]^T\{m_i\}\ .$$

Duhamel's integral can again be employed to obtain the $\{P\}$ vector for $0<t\leqslant\pi t_1$ and for $t\geqslant\pi t_1$. It may be noted here that the solution for $\{P\}$ is obtained in two parts, as in the continuous analysis, one valid for $0<t\leqslant\pi t_1$ and the other for $t\geqslant\pi t_1$, care being taken in the integration limits of the integral. Therefore, for $0<t\leqslant\pi t_1$:

$$\{P\} = -\left[\omega_i\right]^{-1}\int_0^t \left[\sin\omega_i(t-\tau)\right]\frac{A_o\sin(\tau/t_1)}{N\ m}\ [\nu]^T\{m_i\}\ d\tau$$

$$= \frac{-A_o}{2Nm}\left[\omega_i\right]^{-1}\int_0^t \left[\cos(\omega_i t-\omega_i\tau-\tau/t_1)-\cos(\omega_i t-\omega_i\tau+\tau/t_1)\right] \cdot[\nu]^T\{m_i\}\ d\tau$$

$$= \frac{-A_o}{2Nm}\left[\omega_i\right]^{-1}\left[\frac{\sin(\omega_i t-\omega_i\tau-\tau/t_1)}{-(\omega_i+1/t_1)} - \frac{\sin(\omega_i t-\omega_i\tau+\tau/t_1)}{-(\omega_i-1/t_1)}\right]\Bigg|_0^t \cdot[\nu]^T\{m_i\}\ . \qquad (3.19)$$

Further simplification yields:

$$\{P\} = \frac{-A_o}{Nm}[\omega_i]^{-1}\left[\frac{\omega_i \sin(t/t_1) - 1/t_1 \sin(\omega_i t)}{(\omega_i^2 - 1/t_1^2)}\right][\nu]^T\{m_i\} \cdot \tag{3.20}$$

Since $\{\tilde{x}\} = [\nu]\{P\}$, it follows that:

$$\{\tilde{x}\} = \frac{-A_o}{Nm}[\nu][\omega_i]^{-1}\left[\frac{\omega_i \sin(t/t_1) - 1/t_1 \sin(\omega_i t)}{(\omega_i^2 - 1/t_1^2)}\right][\nu]^T\{m_i\} \cdot \tag{3.21}$$

The solution for $t \geq \pi t_1$ is obtained by using the limits of integration from 0 to πt_1 in the eq. (3.19). Therefore, for $t \geq \pi t_1$:

$$\{P\} = \frac{-A_o}{2Nm}[\omega_i]^{-1}\left[\frac{\sin(\omega_i t - \omega_i \tau - \tau/t_1)}{-(\omega_i + 1/t_1)} - \frac{\sin(\omega_i t - \omega_i \tau + \tau/t_1)}{-(\omega_i - 1/t_1)}\right]\Bigg|_0^{\pi t_1}$$

$$\cdot [\nu]^T\{m_i\}$$

is obtained. On simplification:

$$\{P\} = \frac{A_o}{Nm}[\omega_i]^{-1}\left[\frac{\sin\ \omega_i(t - \pi t_1) + \sin(\omega_i t)}{t_1(\omega_i^2 - 1/t_1^2)}\right][\nu]^T\{m_i\} \tag{3.22}$$

is obtained. Since $\{\tilde{x}\} = [\nu]\{P\}$, it follows that:

$$\{\tilde{x}\} = \frac{A_o}{Nm}[\nu][\omega_i]^{-1}\left[\frac{\sin\ \omega_i(t - \pi t_1) + \sin(\omega_i t)}{t_1(\omega_i^2 - 1/t_1^2)}\right][\nu]^T\{m_i\}. \tag{3.23}$$

It is important to note that the period, $2\pi t_1$, of the half sine pulse is changed as in the continuous analysis and depends, now, upon the fundamental period of the lumped parameter model under consideration. The relative mass

displacement vector, $\{\tilde{x}\}$, was evaluated for all the four cases of the period of the half sine pulse, i.e., pulse period 50% less, 10% less, 10% greater and 50% greater than the fundamental period of the system under consideration.

D. Strain Energy Form for Discrete Systems

The strain energy of the lumped parameter models is evaluated for each model and compared with the reference quantity, the strain energy obtained from the continuous analysis. The strain energy for the principal modes and the forced excitation is dealt with in this section.

Principal Modes

The mode shapes of the models evaluated in section B need to be normalized to obtain consistent results with those of the continuum and this is done in a manner similar to the one followed for the continuum.

If D_ν is the normalization constant, it can be evaluated from the relation:

$$D_\nu^2 \{X_\nu\}^T [m] \{X_\nu\} = N\, m$$

where $\{X_\nu\}$ are the mass point displacements amplitude vector, in the νth mode, established for each model and for specific boundary conditions in section B and N m is the total mass of the bar. Thus, the normalized mode shapes are given by:

$$\{U_\nu(x)\} = D_\nu \{X_\nu\} \ .$$

Maximum strain energy for the νth mode is obtained by using the matrix equation:

$$U_{m_{max}} = \frac{1}{2}\{U_\nu(x)\}^T[K]\{U_\nu(x)\}$$

where [K] is the stiffness matrix of the model in question.

Forced Excitations

Strain energy of the lumped parameter models is obtained by using the matrix equation:

$$U_m = \frac{1}{2}\{\tilde{x}\}^T[K]\{\tilde{x}\} \qquad (3.24)$$

where $\{\tilde{x}\}$ is the relative mass point deflections vector of the model and the type of excitation in question. Since $\{\tilde{x}\}$ is time dependent, the maximum value of the system strain energy can be found by computing the strain energy for various values of time 't'. Difference in the maximum strain energy of the models and that of the continuum is checked for convergence and the rate of convergence as a function of N, the number of segments. Results of these comparisons are included in the next chapter.

CHAPTER IV

COMPARISON OF LUMPED PARAMETER MODELS

A. Basis of Comparison

The objective of this study has been to provide a consistent basis of comparison for lumped parameter models of one-dimensional systems in a general dynamic state. The basis chosen for this comparison is the maximum system strain energy as it is indicative of displacements and stresses in the system independent of their position dependence within the system. Furthermore, this basis of model comparison should give a better measure of total system distortion than any one particular parameter, e.g., maximum displacement or maximum stress. The strain energy expressions in principal modes and under forced excitations for the continuum and the lumped parameter models have been derived in chapters II and III, respectively. In this chapter these expressions have been numerically evaluated for the comparison of the models.

For the model comparison a system has been devised whereby the strain energy expressions can be evaluated numerically. In this system

$$\frac{AE}{L} = 1 \text{ , and}$$

$$\rho L = Nm = 1 \text{ .}$$

$$\therefore \quad \frac{a}{L} = \sqrt{\frac{AE}{\rho L^2}} = 1 \text{ .}$$

For the same reason, it is assumed that the amplitude, A_o of the base acceleration is also equal to unity.

It may be mentioned here that in the evaluation of the comparisons of the lumped parameter models, the strain energy value obtained from the exact solution (continuous) will always be utilized as the reference point.

B. Comparisons in Principal Modes

The maximum system strain energy in the νth mode, of the continuum with fixed-fixed ends is obtained from eq. (2.45) and with the constants chosen simplifies to:

$$U_{c_{max}} = \frac{1}{2}(\nu\pi)^2 \ .$$

For fixed-free ends, the maximum strain energy is obtained from eq. (2.47) which reduces to the form:

$$U_{c_{max}} = \frac{1}{8}[(2\nu-1)\pi]^2 \ .$$

The maximum system strain energy in the νth mode, of the lumped parameter models with any specific boundary conditions, is found from the relation:

$$U_{m_{max}} = \frac{1}{2}\{U_\nu(x)\}^T[K]\{U_\nu(x)\} \ .$$

The normalized eigenvectors, $\{U_\nu(x)\}$, for the νth mode of the models are obtained for a specific boundary condition as explained earlier in chapter III.

Figure 7a shows the behavior of the difference in maximum strain energy of the continuous system and that of the models (a) and (c) as a function of the number of segments, N, for the first three modes with boundary conditions as fixed-fixed. The corresponding difference for model (b) is shown in fig. 7b.

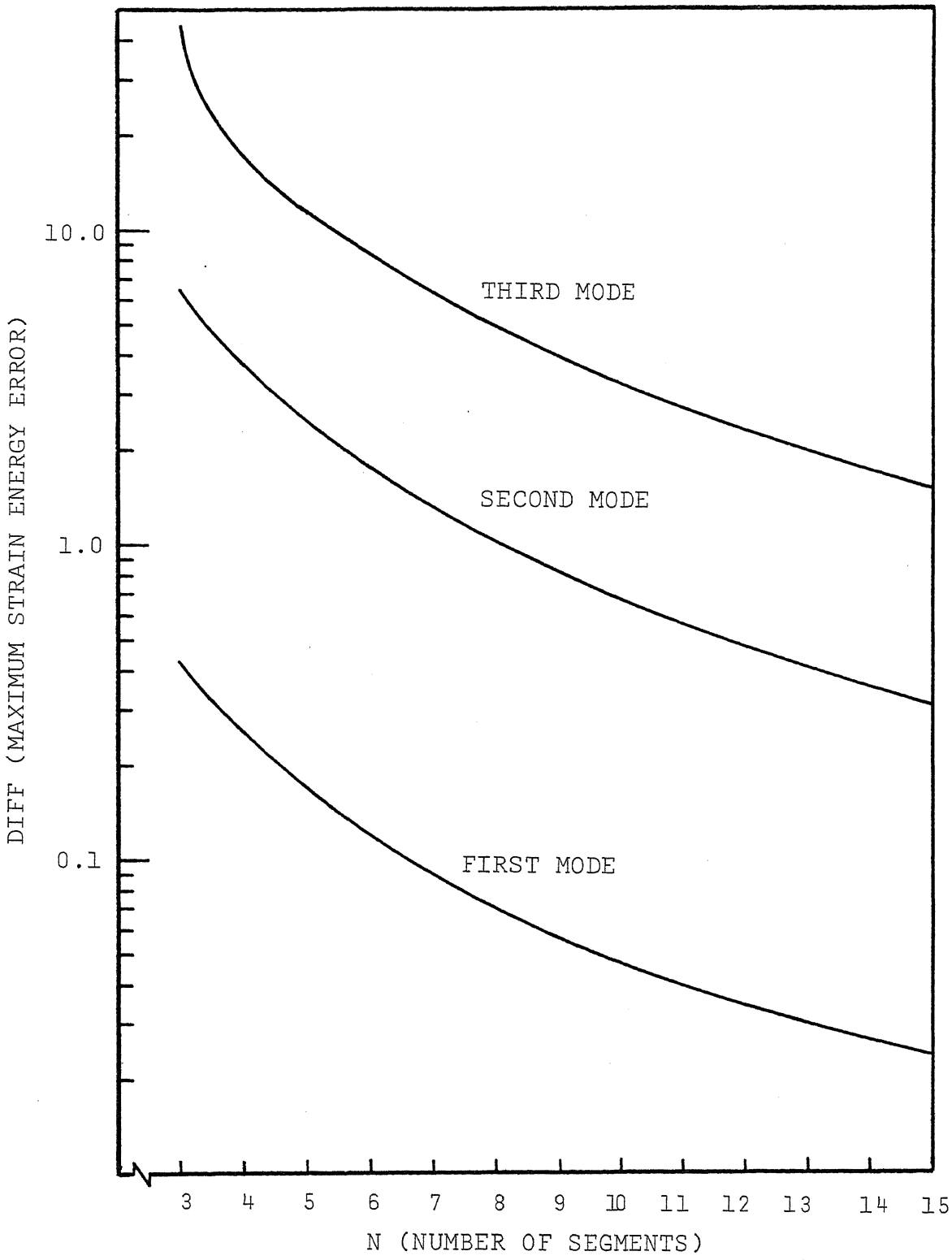

Fig. 7a Maximum Strain Energy Errors for Models (a) and (c) with Fixed-Fixed Boundary Conditions

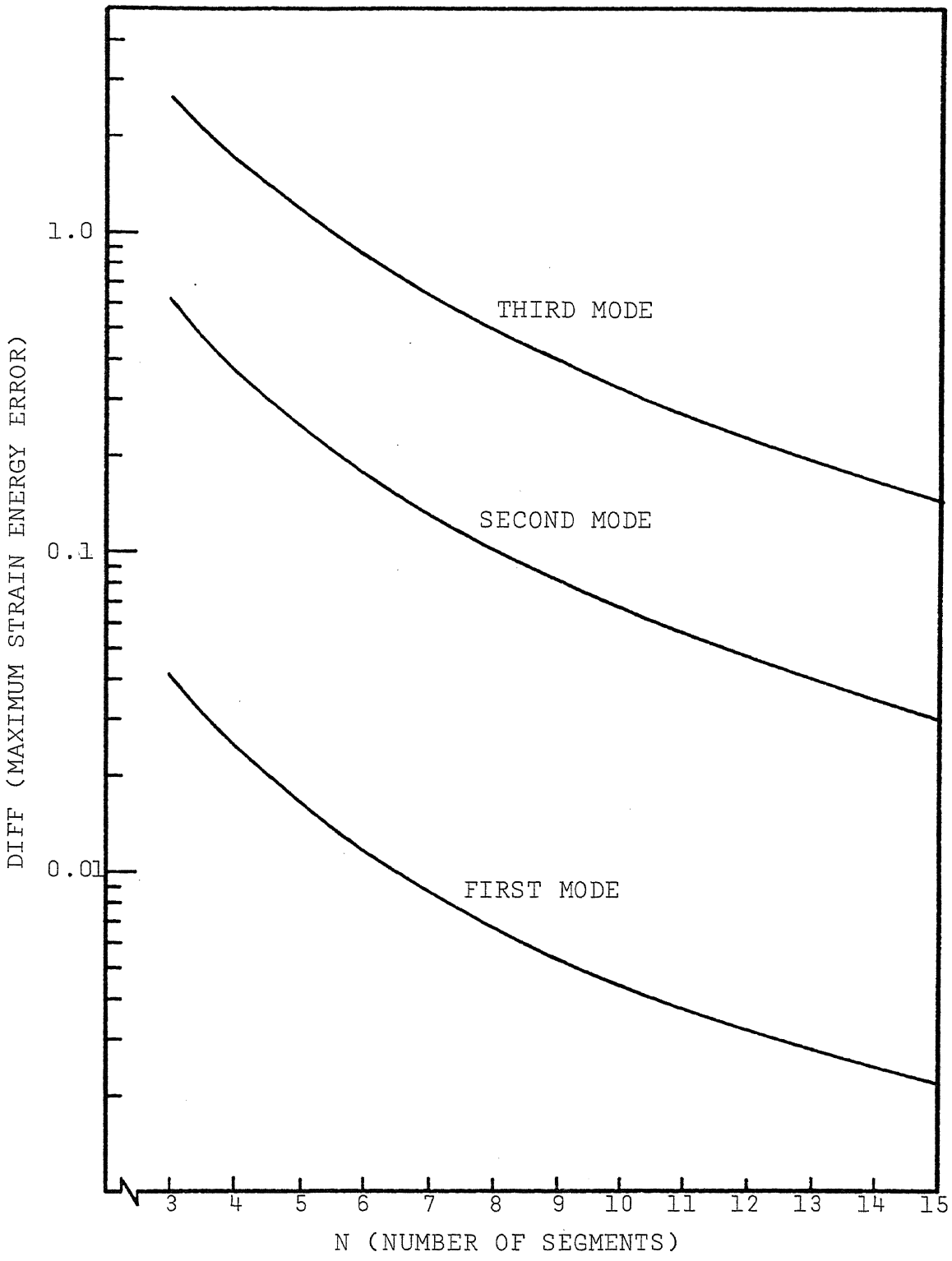

Fig. 7b Maximum Strain Energy Errors for Model (b) with Fixed-Fixed Boundary Conditions

Figures 7c, 7d and 7e show the difference in maximum strain energy of the continuous systems and that of the models (a), (b) and (c) respectively, for the first three modes with fixed-free boundary conditions.

Models (a) and (b) are found to behave as $\frac{1}{N^2}$ for a large value of N for both fixed-fixed and fixed-free ends. This is established numerically as shown below: (refer to the curve in the second mode of fig. 7c).

At N = 15, DIFF, the difference in maximum strain energy, is equal to 0.094. Assuming the relation:

$$DIFF = \alpha/N^2$$

$$0.094 = \alpha/225, \text{ or}$$

$$\alpha = 0.094 \times 225 \text{ is obtained.}$$

Assuming the form above, DIFF at N = 10 should be:

$$DIFF = 0.094 \times 225/100$$

$$= 0.2118.$$

From the graph at N = 10, DIFF is found to be 0.208. Therefore, at these values of N the results follow closely the assumed form. To check the accuracy of the assumed behavior for small values of N, the value of DIFF = 2.10 is obtained from the graph at N = 3 and by calculation, it is found to be:

$$DIFF = 0.094 \times 225/9 = 2.35.$$

It can, therefore, be seen that the assumed behavior is in error by 11.9%, for small values of N. This is still close for engineering guideline purposes.

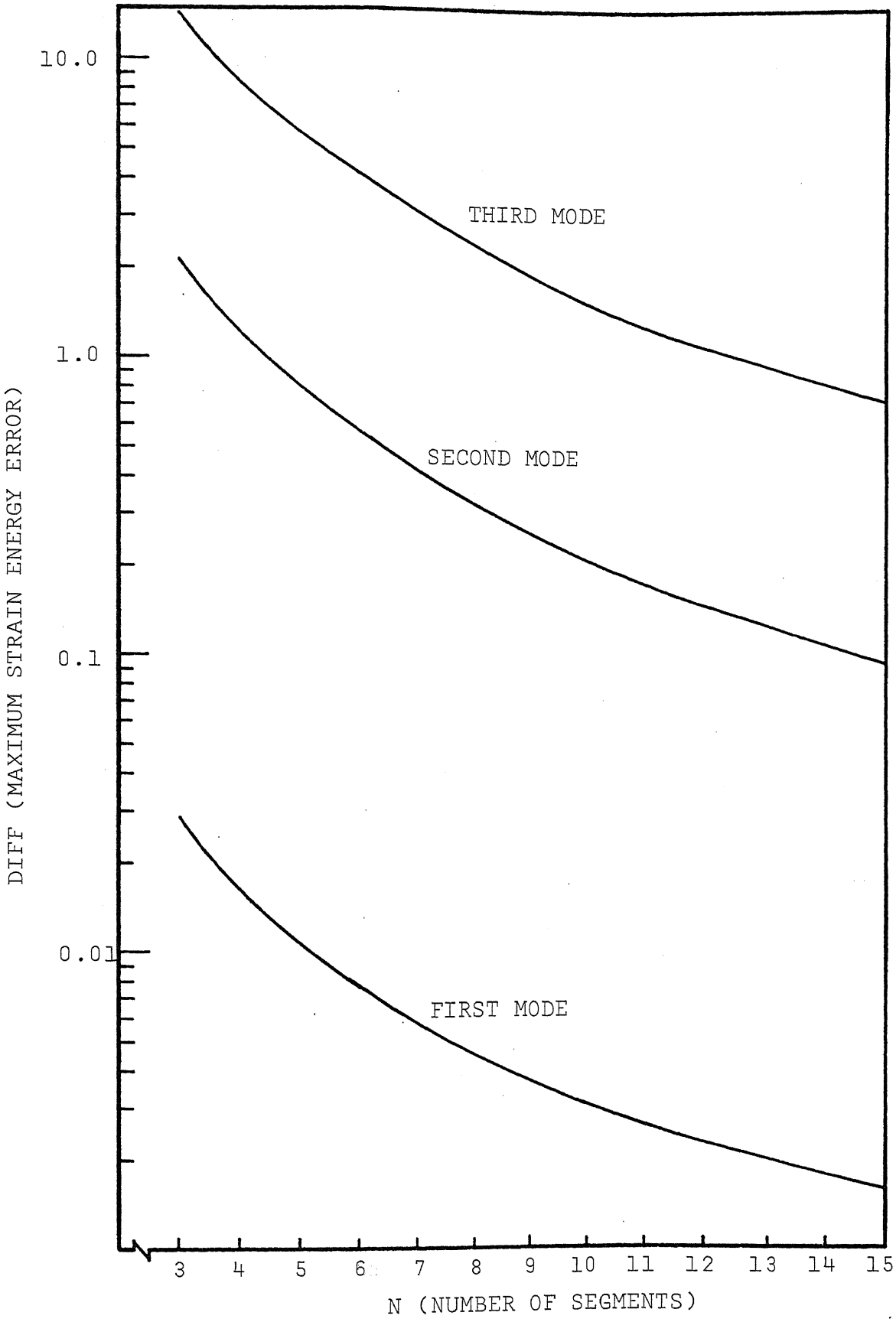

Fig. 7c Maximum Strain Energy Errors for Model (a) with Fixed-Free Boundary Conditions

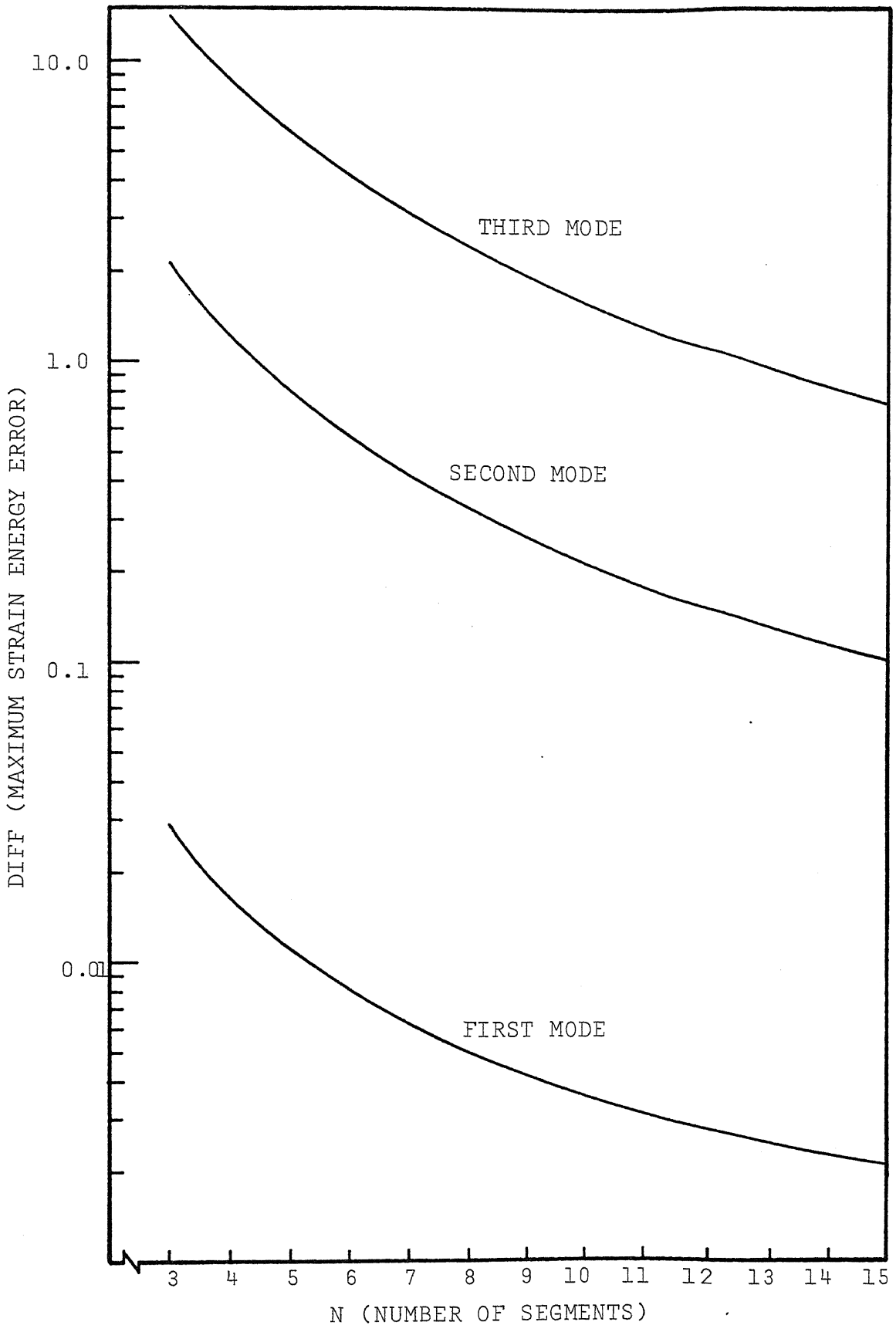

Fig. 7d Maximum Strain Energy Errors for Model (b) with Fixed-Free Boundary Conditions

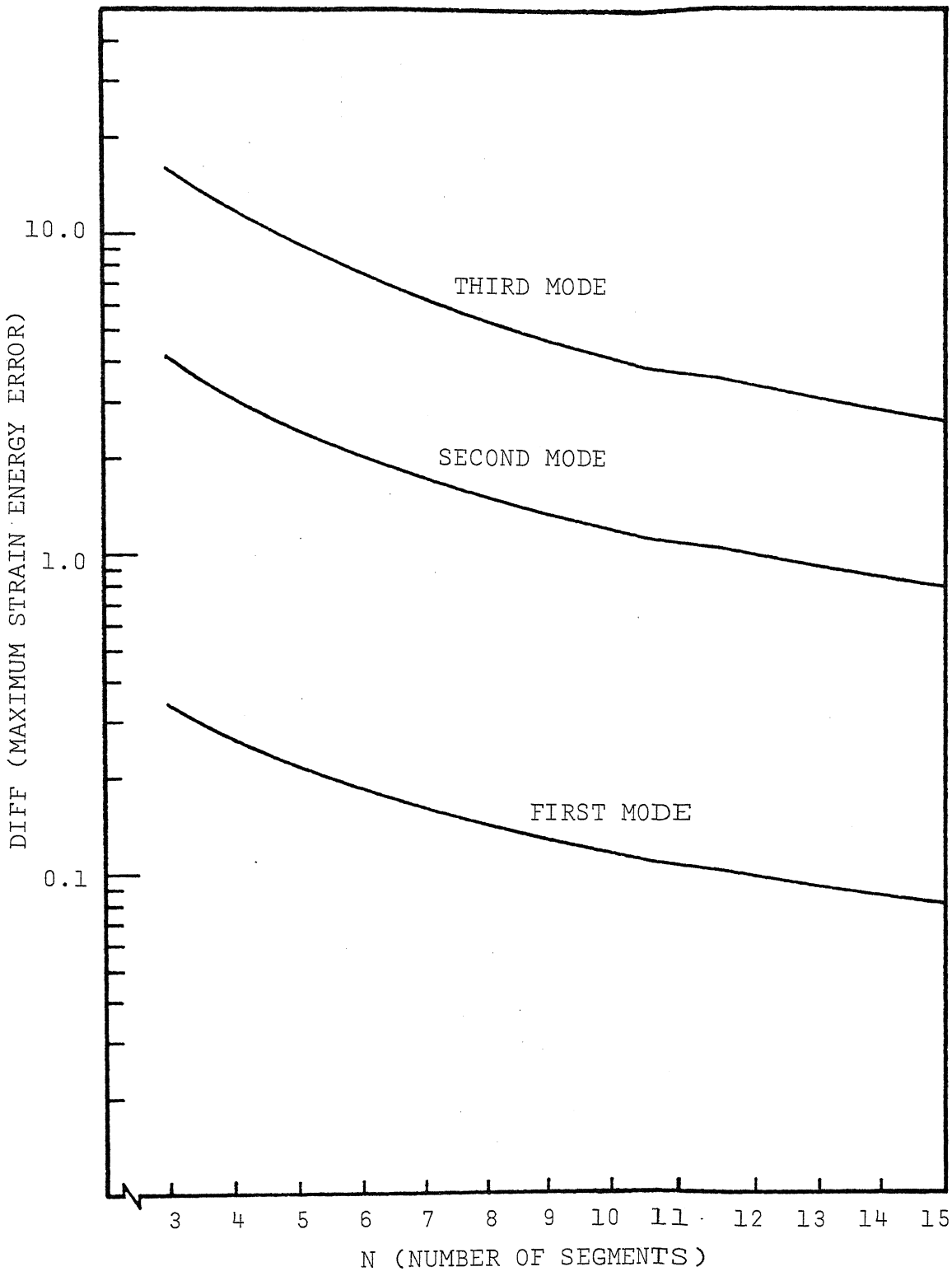

Fig. 7e Maximum Strain Energy Errors for Model (c) with Fixed-Free Boundary Conditions

Similarly, for models (a) and (c), the results for small N are found to be in error by about 15.4% with fixed-fixed ends. For model (b) the corresponding percentage is found to be 19 with fixed-fixed ends and 17.9 with fixed-free ends. Model (c) behaves as 1/N, for large N, with fixed-free ends and the error in this behavior, for small N, is found to be about 3.66%. This result can also be established numerically as shown above for model (a).

On the basis of the above discussion it can be concluded that models (a) and (b) give more consistent errors in strain-energy approximation for the specific boundary conditions used. It may be noted also that models (a) and (c) have only (N-1) differential equations to work with for fixed-fixed boundary conditions while model (b) has N.

Previous comparisons[5] based on the frequency root errors have established similar results obtained here by using the strain energy comparison. The error in the maximum strain energy representation behaves similar to the frequency root errors for models (a), (b) and (c) for the boundary conditions considered.

C. Comparison under Forced Excitations

Constant Base Acceleration

To check the numerical calculations against previous work[2], comparison of the models is made on the basis of maximum relative end deflection and the maximum base stress in the system.

The maximum relative end deflection for the continuous system is obtained from the eq. (2.32) after further simplification to:

$$u_R(L,t)_{max} = \frac{-32}{\pi^3} \sum_{n=1,3,5,----} 1/n^3 \sin(n\pi/2)$$
$$= -1.0 \ . \qquad (4.1)$$

The maximum base stress for the continuous systems is obtained from the eq. (2.33) which is simplified to the form,

$$\sigma(0,t)_{max} = -2/A$$

and the maximum base stress per unit cross-sectional area of the bar is given by:

$$\sigma(0,t)_{max} = -2.00 \ . \qquad (4.2)$$

The maximum strain energy of the continuous system is established by using eq. (2.49) after further simplification to obtain:

$$U_{c_{max}} = \frac{64}{\pi^4} \sum_{n=1,3,5,----} 1/n^4 = \frac{2}{3} \ . \qquad (4.3)$$

Relative end deflections for the lumped parameter models are computed from the eq. (3.18) simplified to the form:

$$\{\tilde{x}\} = -[\nu]\left[\omega_i\right]^{-1}\left[\frac{1-\cos(\omega_i t)}{\omega_i}\right][\nu]^T\{m_i\} \ . \qquad (4.4)$$

The peak value for $\tilde{x}_N$ is obtained by computing the vector $\{\tilde{x}\}$ for various values of time 't'. This has been done for N = 3, 5 and 9. Base stresses, for the models with N = 3, 5 and 9 are computed from the expression,

Base stress per unit cross-sectional area of the bar = $(\tilde{x}_2)$ x (stiffness of the first spring from the fixed end) .

$\tilde{x}_2$ is found for various values of time 't' and thus maximum base stress and its timing are established.

Strain energy of the models is calculated from the equation

$$U_m = \frac{1}{2}\{\tilde{x}\}^T [K]\{\tilde{x}\} .$$

Maximum values of strain energy of the three models have been evaluated by computing the strain energy of the models for various values of the time 't'. Difference in the maximum value of the strain energy, between the continuum and that of the models, is found for N = 3, 5 and 9. Values of N as 3, 5 and 9 are chosen to establish the rate of convergence for the low as well as larger values of N.

Figure 8 shows a plot of the relative end deflections against time 't' for models (a), (b) and (c) with fixed-free ends and a constant base acceleration A_o = 1, at the fixed end. Model (a) behaves better than models (b) and (c) on comparison with the continuum, since the peak amplitude of the relative end deflection and its timing are better approximated by model (a). The number of segments considered in fig. 8 is nine while those published[2] for the similar case were made with N = 5. The results with N = 9 show improvement in approximating the peak displacement and its timing over the ones with N = 5.

A plot is drawn for the base stresses against time 't' for the three models with the number of segments considered for

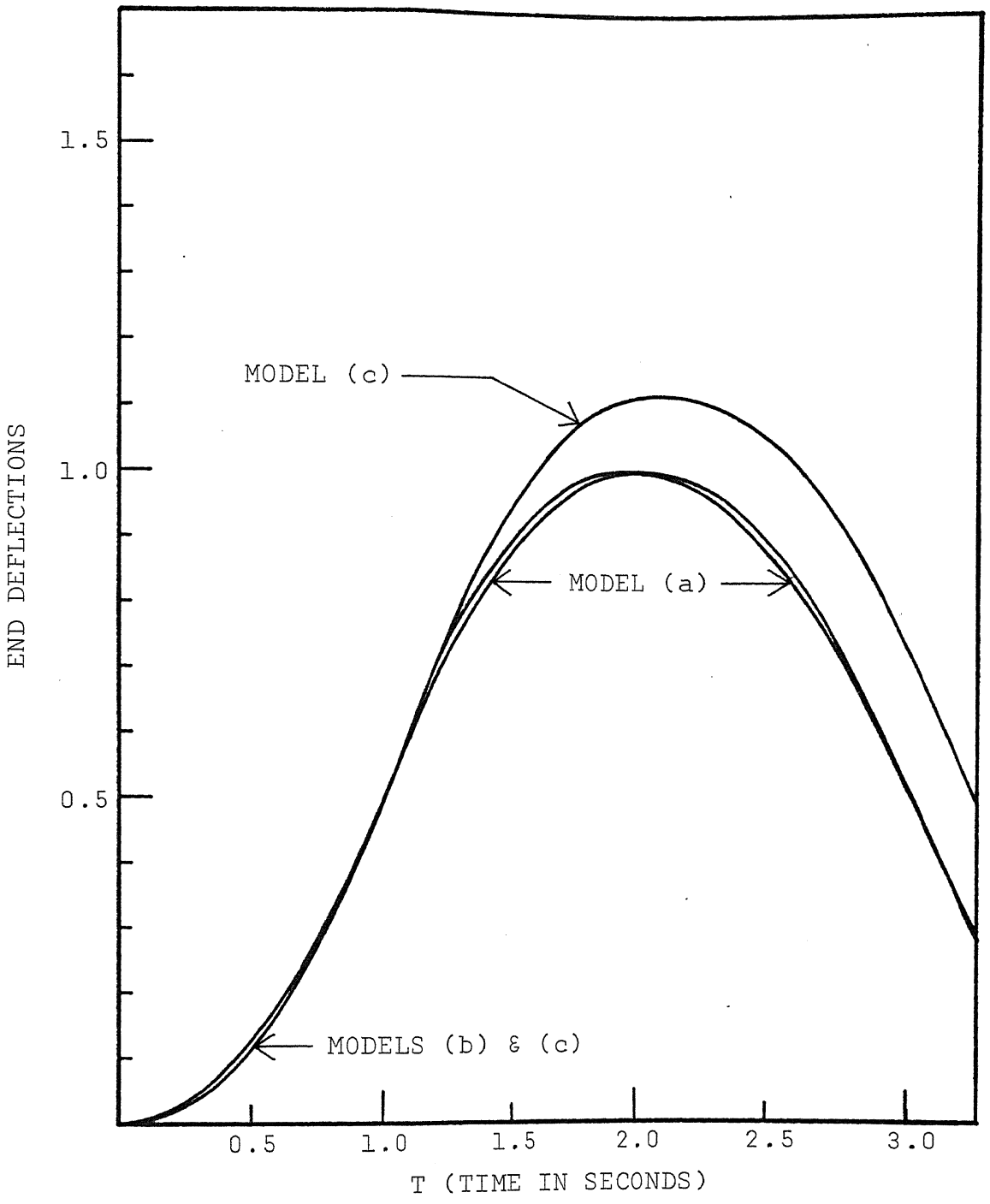

Fig. 8 End Deflections for Models (a), (b) and (c) with Constant Base Acceleration

each model as nine, see fig. 9. Plots with N = 9 show improvement in approximating the continuum as N is increased, as compared to the previous work published[2] with N = 5. The main point being that the results are very close and, thus, verification of the calculations was shown.

Figure 9 shows a plot of the base stress against time 't' for models (a), (b) and (c). The peak amplitude of the stresses is best approximated by models (b) and (c); however, models (a) and (b) are better in approximating the timing of the peak amplitude of the base stresses.

Figure 10 shows a plot of the difference in the maximum strain energy of the continuum and that of the models for constant base acceleration against the number of segments N. Model (a) shows best approximation of the maximum strain energy of the continuum followed by models (b) and (c). The timing for the maximum strain energy is also best approximated by model (a) followed by model (b). Model (c) deviates by 0.1 seconds from the exact timing for the case N = 9. Models (a) and (b) give solutions that agree with the exact solution within the ±0.05 seconds time increment used.

Model (c) behaves as 1/N, for the region of N considered, which is found numerically from the plot, in fig. 10, in a manner similar to the one shown earlier in section B of this chapter. Model (b) behaves slightly better than 1/N and model (a) slightly better than $1/N^2$ for values of N considered. The percentage error for N = 3 (small values of N) in the above behavior for model (b) is about 21% and for model (a) is about

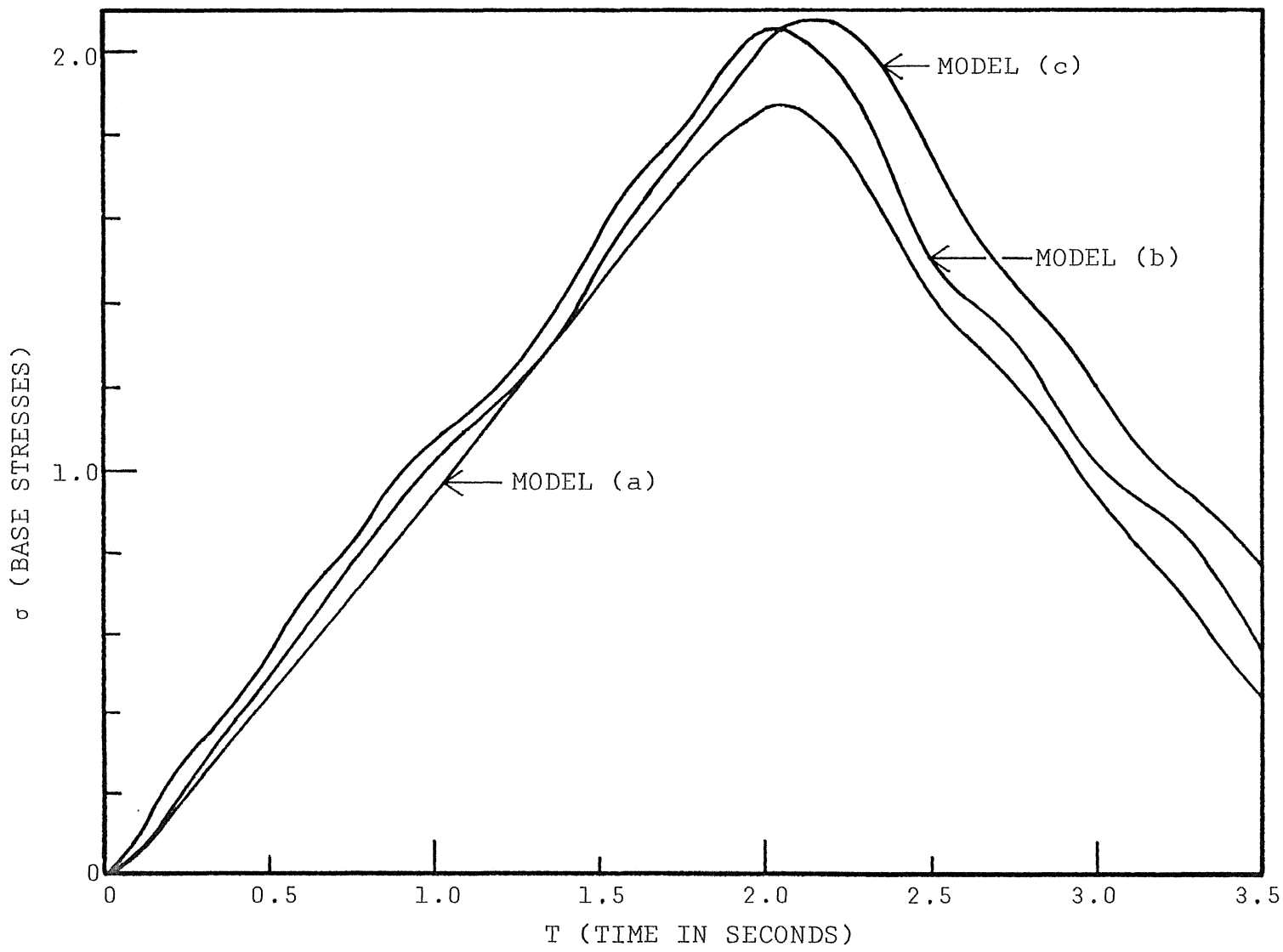

Fig. 9 Base Stresses for Models (a), (b) and (c) with Constant Base Acceleration

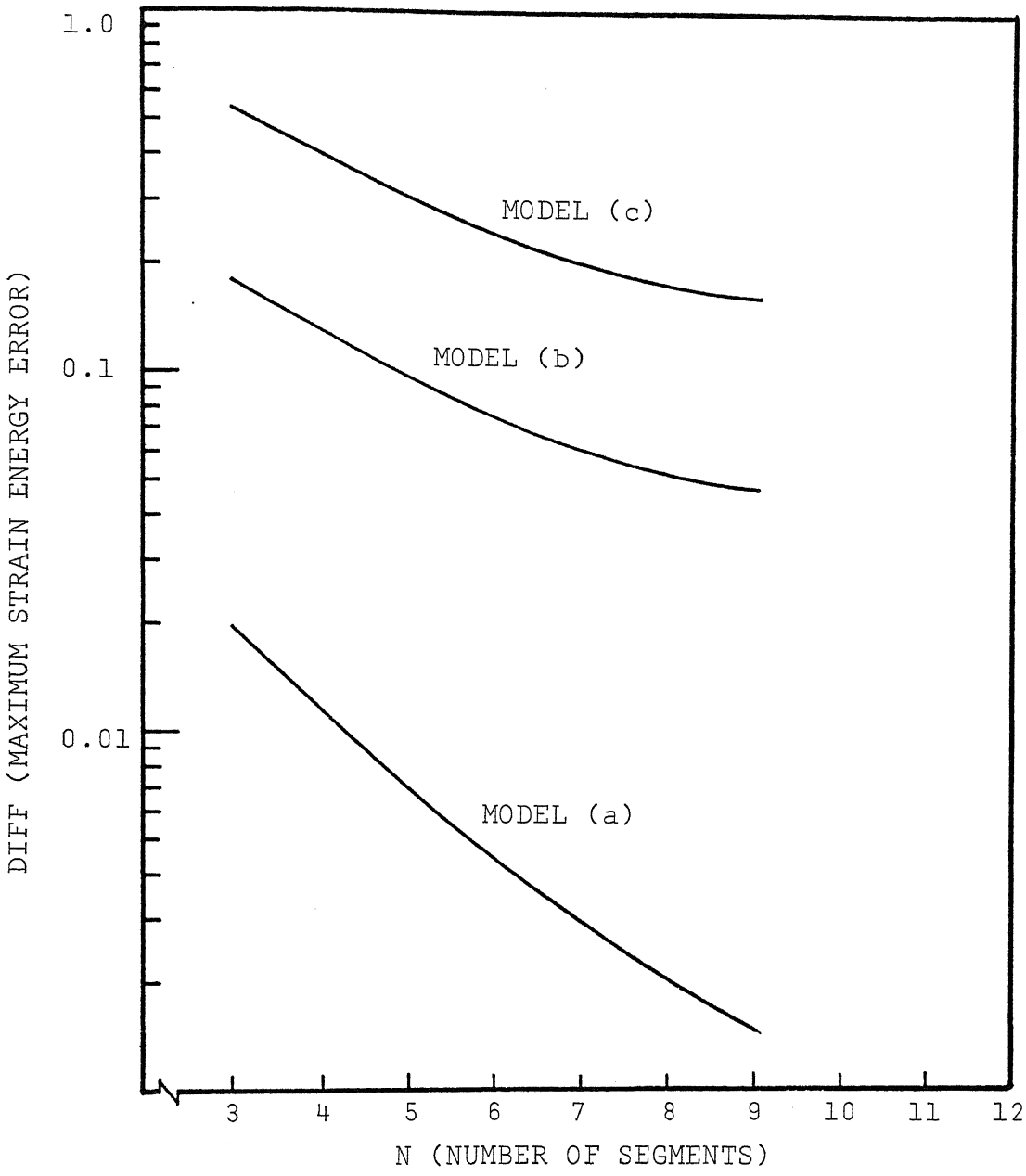

Fig. 10 Maximum Strain Energy Errors for Models (a), (b) and (c) with Constant Base Acceleration

33%. The above behavior are good for the boundary conditions considered, i.e., fixed-free.

These comparisons show that model (a), in general, is better than the other models for the boundary conditions used and for the constant base acceleration problem. It shows more consistent errors on a comparison of maximum strain energy.

Half Sine Pulse Base Acceleration

The maximum strain energy of the continuum is found by evaluating eqs. (2.50) and (2.51) for various values of time 't'. The maximum strain energy may occur in the region $0<t\leq\pi t_1$ or in the region $t\geq\pi t_1$. This, therefore, necessitates the computation of both eqs. (2.50) and (2.51).

These equations for the system under consideration can be rewritten as:

For $0<t\leq\pi t_1$,

$$U_c = \frac{4}{\pi^2}\sum_{n=1,3,5,----} 1/n^2 \cdot \frac{\left[\frac{n\pi}{2}\sin(t/t_1)-1/t_1\sin(\frac{n\pi t}{2})\right]^2}{\{(\frac{n\pi}{2})^2-1/t_1^2\}^2} \qquad (4.5)$$

and for $t\geq\pi t_1$,

$$U_c = \frac{4}{\pi^2 t_1^2}\sum_{n=1,3,5,----} 1/n^2 \cdot \frac{\left[\sin\{\frac{n\pi}{2}(t-\pi t_1)\}+\sin(n\pi t/2)\right]^2}{\{(\frac{n\pi}{2})^2-1/t_1^2\}^2} \cdot \qquad (4.6)$$

Maximum strain energy for the continuum is established for all values of t_1 discussed in chapter II from eqs. (2.50) and (2.51). Maximum strain energy of the three models under consideration is obtained from the equation:

$$U_m = \frac{1}{2}\{\tilde{x}\}^T[K]\{\tilde{x}\} \cdot \qquad (4.7)$$

The vector $\{\tilde{x}\}$ can be established from eqs. (3.21) and (3.23) for $0<t\leqslant\pi t_1$ and $t\geqslant\pi t_1$, respectively. For a system with AE/L=1 and N m=1, these equations become:

For $0<t\leqslant\pi t_1$,

$$\{\tilde{x}\} = [\nu]\lceil\omega_i\rfloor^{-1}\left[\frac{\omega_i\sin(t/t_1)-1/t_1\sin(\omega_i t)}{(\omega_i^{\,2}-1/t_1^{\,2})}\right][\nu]^T\{m_i\} \tag{4.8}$$

and for $t\geqslant\pi t_1$,

$$\{\tilde{x}\} = [\nu]\lceil\omega_i\rfloor^{-1}\left[\frac{\sin\omega_i(t-\pi t_1)+\sin(\omega_i t)}{t_1(\omega_i^{\,2}-1/t_1^{\,2})}\right][\nu]^T\{m_i\}\ . \tag{4.9}$$

Equations (4.8) and (4.9) are used in eq. (4.7) to provide continuity through the point $t=\pi t_1$, and the strain energy is computed for different values of time 't'. This gives the maximum strain energy of the system at a particular value of time 't'.

Likewise, maximum strain energy for the three models is established for the four values of t_1 discussed earlier. The procedure is repeated with N = 3, 5 and 9. Difference in the maximum strain energy of the continuum and that of the models was found and plotted against the number of segments, N, of the model. This was done for the four values of t_1.

Figure 11a shows a plot of the difference in the maximum strain energy of the continuum and that of the models (a), (b) and (c) as a function of N with $t_1 = \frac{0.5}{\omega_1}$. Figures 11b, 11c and 11d show similar results with $t_1 = \frac{0.9}{\omega_1}$, $t_1 = \frac{1.1}{\omega_1}$ and $t_1 = \frac{1.5}{\omega_1}$, respectively. In all four plots model (a)

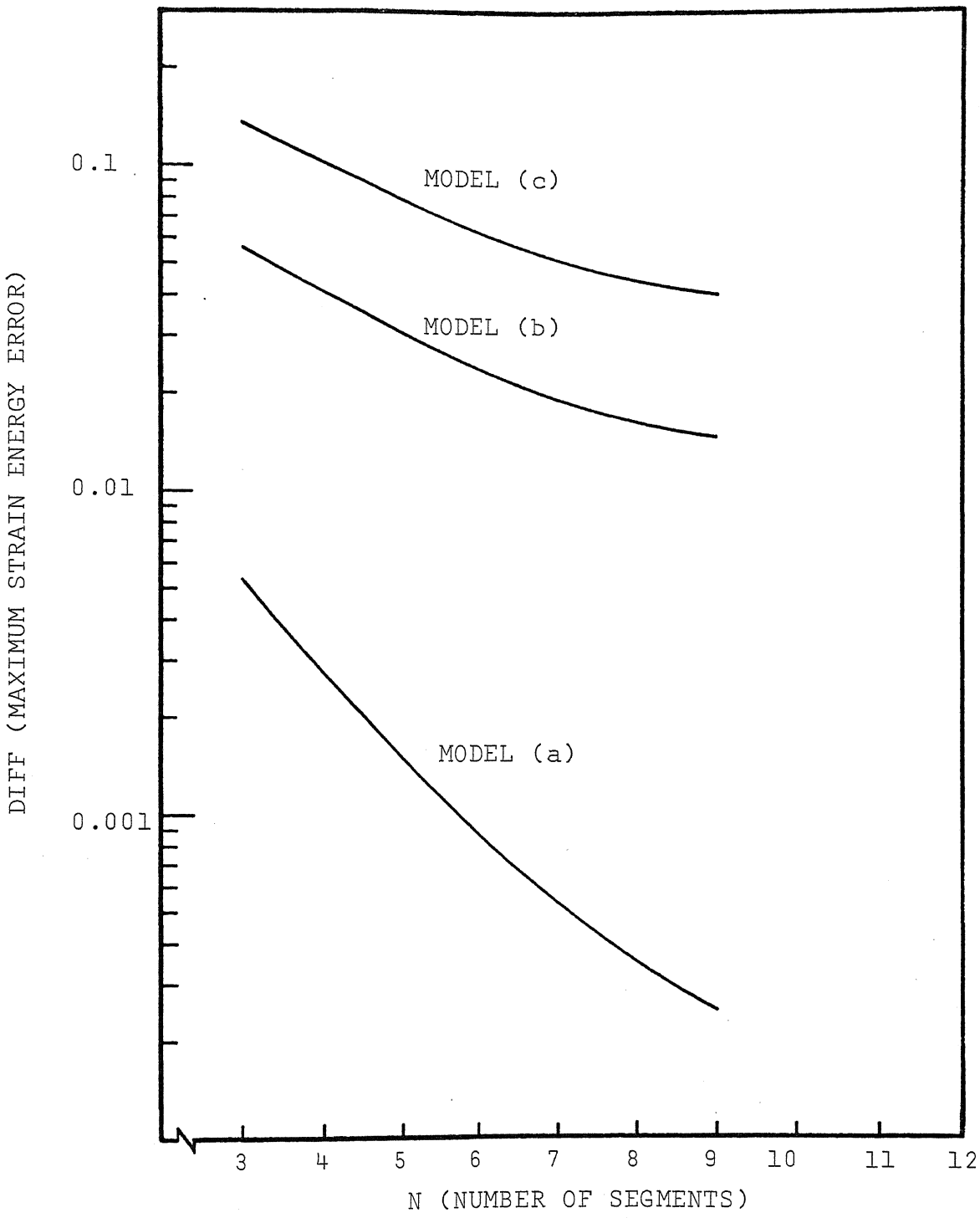

Fig. 11a Maximum Strain Energy Errors for Models (a), (b) and (c) with Half Sine Pulse Base Acceleration (Duration equals 25% of the fundamental period of the system)

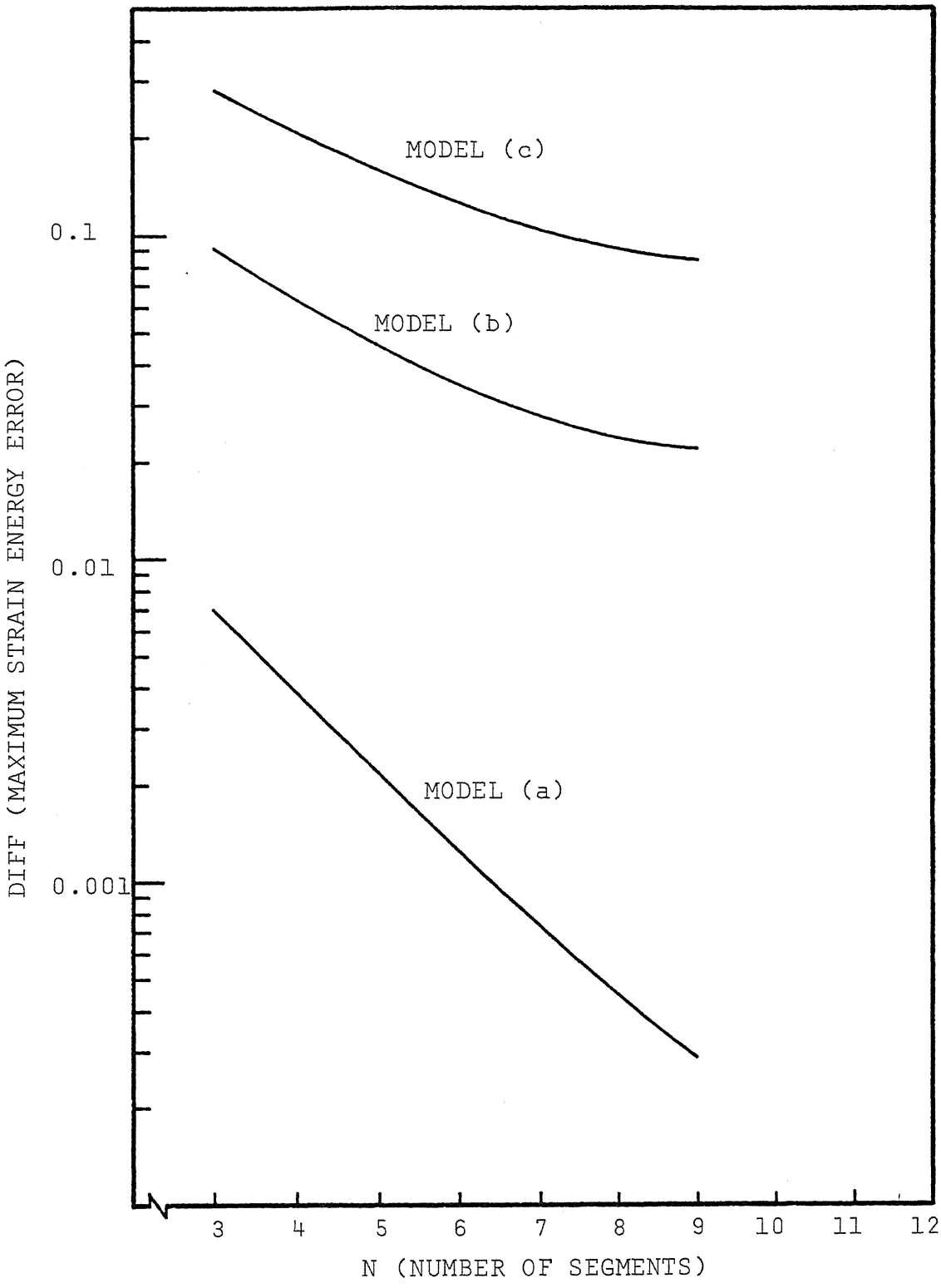

Fig. 11b Maximum Strain Energy Errors for Models (a), (b) and (c) with Half Sine Pulse Base Acceleration (Duration equals 45% of the fundamental period of the system)

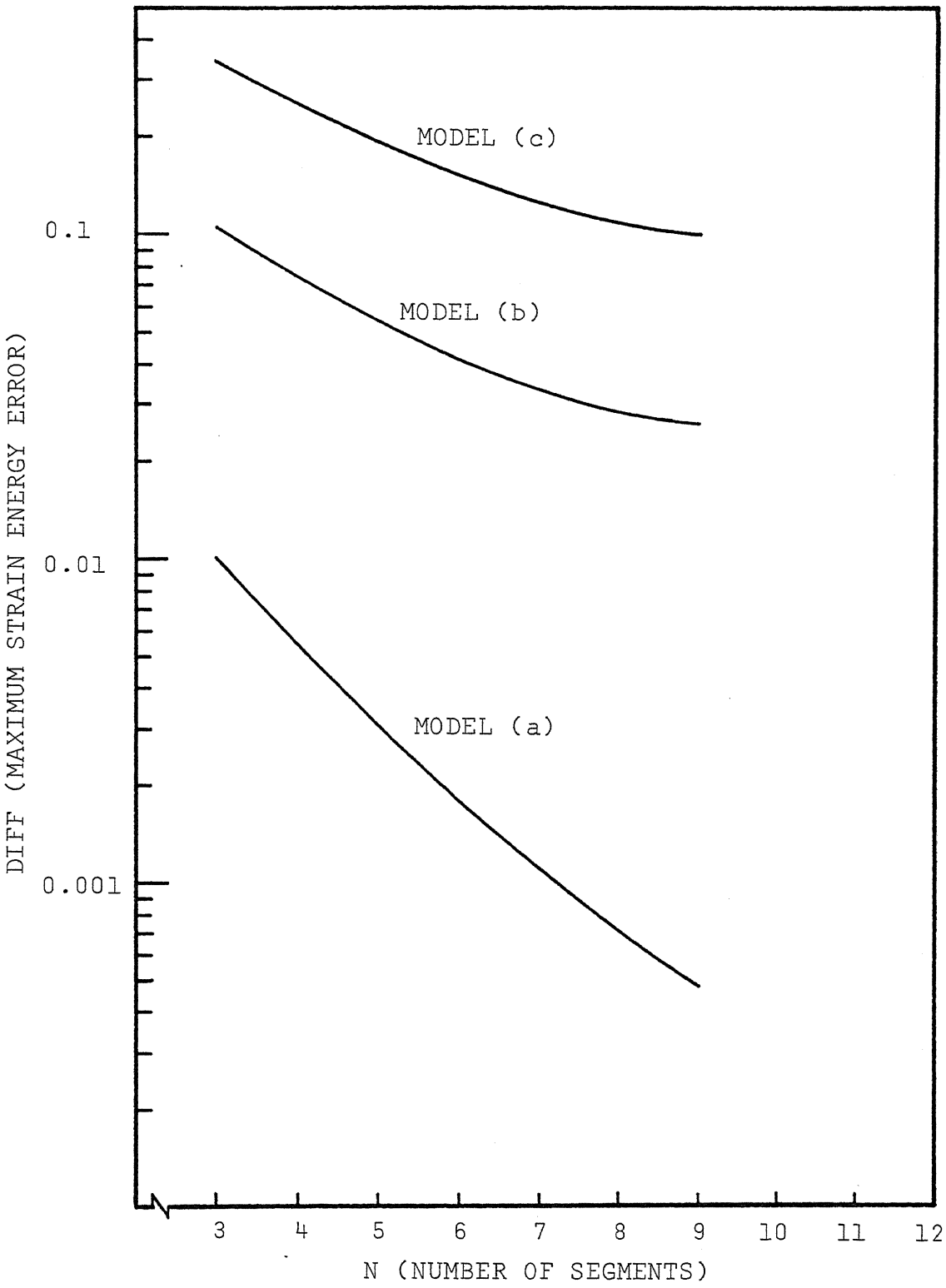

Fig. 11c Maximum Strain Energy Errors for Models (a), (b) and (c) with Half Sine Pulse Base Acceleration (Duration equals 55% of the fundamental period of the system)

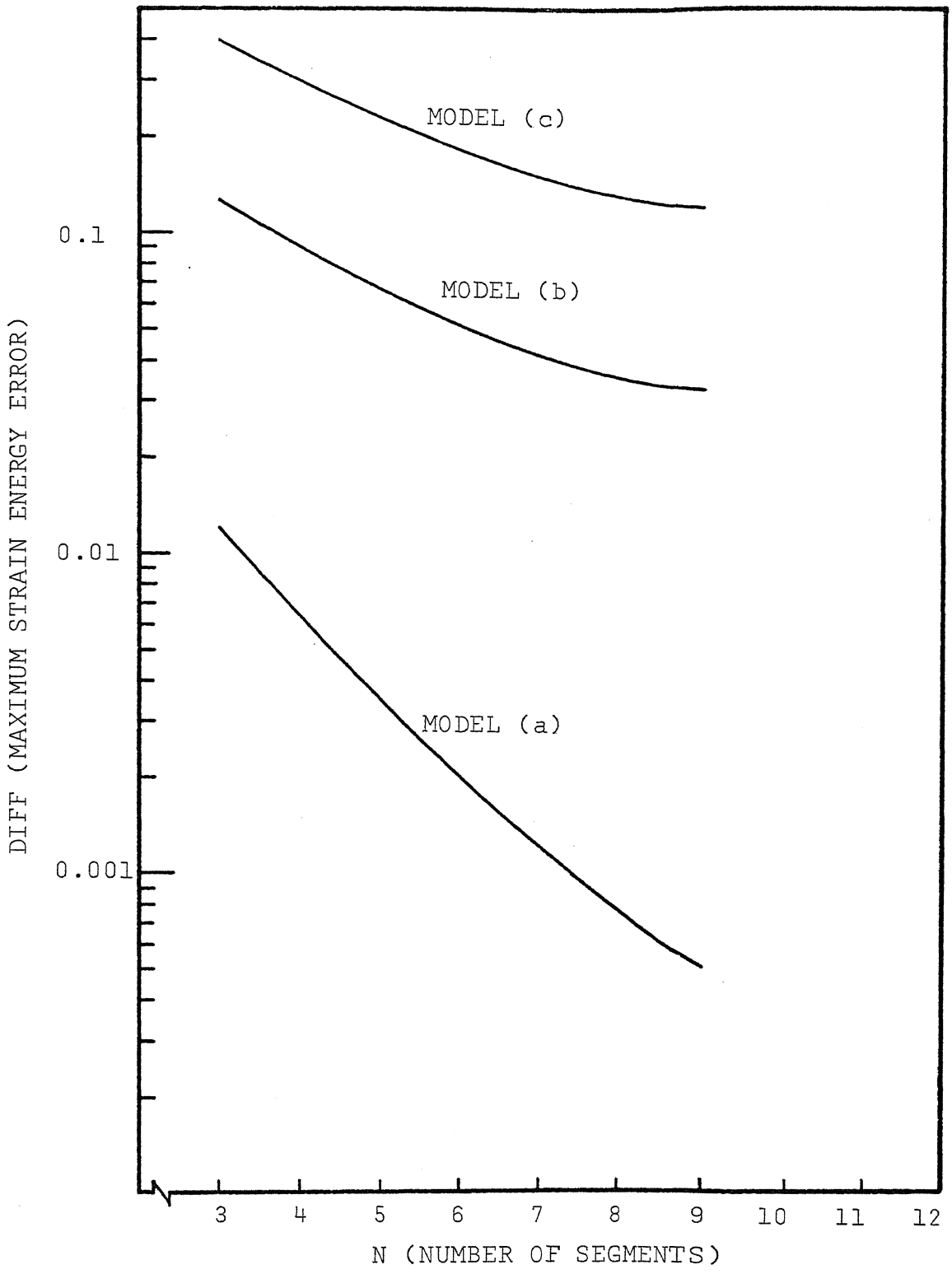

Fig. 11d Maximum Strain Energy Errors for Models (a), (b) and (c) with Half Sine Pulse Base Acceleration (Duration equals 75% of the fundamental period of the system)

behaves approximately as $\frac{1}{N^3}$ for the values of N considered as 3, 5 and 9. For a small value of N, the percentage error in the above behavior is about 28%. Model (b) behaves nearly as $\frac{1}{N}$ for the region of N considered and for all the four plots. The error in the behavior for a small value of N is about 23.7%. Model (c) behaves approximately as $\frac{1}{N}$ for all the four cases of the pulse duration. The error in the behavior for a small value of N is about 9.6%.

Note that the above behavior of models (a), (b) and (c) are good for the fixed-free ends with base acceleration applied at the fixed end only. As discussed earlier, however, this result is analogous to the system with fixed free ends and a uniformly distributed time dependent forcing function.

As can be seen from the plots for $t_1 = 0.9/\omega_1$ and $t_1 = 1.1/\omega_1$ the maximum strain energy is finite and is, therefore, also expected to be finite for the case where $t_1 = \frac{1}{\omega_1}$, i.e., for the time period of the half sine pulse to be exactly equal to the fundamental period of the system. Equations (2.50), (2.51), (3.21) and (3.23) are all indeterminate for this particular case where $t_1 = \frac{1}{\omega_1}$. By applying La-Hospital's rule to these equations it was found that the strain energy of the system, for the case when $t_1 = 1/\omega_1$, is bounded and the value of the maximum strain energy, for this case, can be established. The evaluation of the strain energy of the system in the case of $t_1 = \frac{1}{\omega_1}$ was not found necessary due to the complications involved in its computation. Instead the two border cases of $t_1 = 0.9/\omega_1$ and $t_1 = 1.1/\omega_1$ were examined.

The duration of the half sine pulse was a function of the model being investigated and was determined as a percentage of the period of the fundamental mode of each model. The variation in the duration of the pulse was not appreciable from model to model. This change does not effect the absolute value of the maximum system strain energy appreciably as can be seen from the maximum system energy error curves for the half sine pulse. Examining these curves for any given model shows that the maximum strain energy difference between models varies slightly when t_1 is changed by a factor of three, which is represented by a change of 25% to 75% of the fundamental period.

Since the pulse duration was varied from model to model, no correlation could be obtained for the time occurrence of the maximum strain energy. This correlation could have been obtained if the pulse duration had been held constant for all models. One means of doing this would be to select the pulse duration as a percentage of the duration of the fundamental mode of the continuous system.

CHAPTER V

CONCLUSIONS

Using the maximum strain energy as a basis of comparison, several conclusions can be reached about the accuracies of the three lumped parameter models examined.

1. Model (a) (mass-spring-mass) and model (b) (spring-mass-spring) produce essentially equivalent strain energy errors in the principal modes. When N is large, the errors behave as $1/N^2$ in the principal modes with fixed-fixed and fixed-free end conditions.

2. Model (c) (spring-mass) is less consistent than models (a) and (b) under the same principal mode comparison. For fixed-fixed ends, the strain energy error behavior is $1/N^2$ for a large value of N and for fixed-free ends it is found to be $1/N$, when N is large. The behavior of all the three models is similar to that based on the frequency root error comparison.

3. It is possible to formulate a related system of models with base acceleration by a change to relative coordinates. Thus all results derived in the study are equally applicable to systems with uniformly distributed forcing functions.

4. In extending the model comparisons to transient behavior, models (a) and (b) were found to produce more consistent strain energy error for both the constant base acceleration and the half sine pulse base acceleration types of excitation. For the constant base acceleration, models (a) and (b) behave approximately as $1/N^2$ while the behavior for model (c) is

found to vary approximately as 1/N for values of N in the range 3, 5 and 9. This result is similar to that of the frequency root error behavior obtained by Rocke[2].

5. In the case of half sine pulse type of excitation, model (a) with fixed-free ends is found to behave approximately as $1/N^3$ for values of N considered being 3, 5 and 9. Under the same comparison, the behavior for model (b) varies slightly better than $1/N^2$ and that for model (c) slightly better than 1/N.

6. The timing for the maximum system strain energy for the constant base acceleration problem is best approximated by model (a). Model (b) is less accurate and model (c) deviates considerably from the exact timing.

CHAPTER VI

APPENDIX A

DERIVATION OF THE DIFFERENCE EQUATION

Frequently in a dynamical system identical sections are repeated several times. The equations of motion can then be treated with advantage by the difference equation. As an example of repeating sections, consider the N-segments spring-mass system (fig. 12), where all masses are equal to m and all springs have a stiffness of K. The differential equation of motion for the Nth mass is then:

$$m\ddot{x}_N = K(x_{N+1}-x_N)-K(x_N-x_{N-1}) \quad . \qquad (A\text{-}1)$$

Assuming harmonic motion of the masses, i.e., let form of solution be:

$$x_n = X_n e^{i\omega t} \quad . \qquad (A\text{-}2)$$

Substituting eq. (A-2) in eq. (A-1), eq. (A-1) becomes:

$$X_{N+1}-2\left(1-\frac{m\omega^2}{2K}\right)X_N+X_{N-1} = 0 \quad . \qquad (A\text{-}3)$$

This suggests form of solution for X_n as:

$$X_n = e^{i\beta n} \qquad (A\text{-}4)$$

which leads to the relationship:

$$\left(1-\frac{m\omega^2}{2K}\right) = \frac{e^{i\beta}+e^{-i\beta}}{2} = \cos\beta . \qquad (A\text{-}5)$$

From eq. (A-4), the general solution for X_n is given by:

$$X_n = A\cos(\beta n) + B\sin(\beta n)$$

where: A and B are constants.

Note that β, a parameter dependent upon the symmetrical properties m and K and the natural frequency of the system is evaluated from the boundary conditions in the given problem.

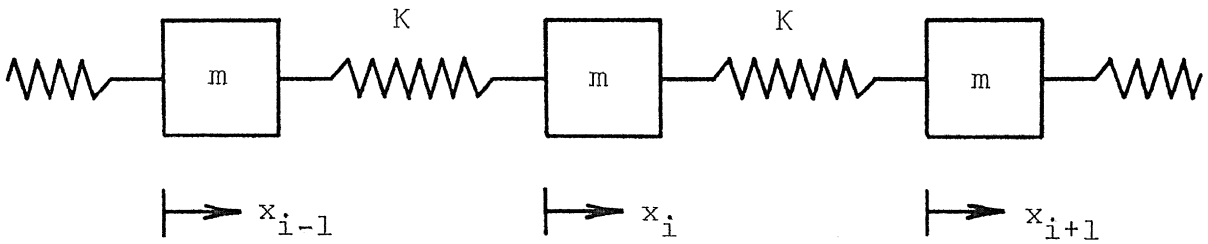

Fig. 12 Spring-Mass System with N Symmetrical Segments

CHAPTER VII

BIBLIOGRAPHY

1. Duncan, W., "A Critical Examination of the Representation of Massive and Elastic Bodies by Rigid Masses Elastically Connected", Quarterly Journal of Mechanics and Applied Mathematics, Vol. 5 (1952) pp. 97-108.

2. Rocke, R. D., "Comparison of Lumped Parameter Models Commonly Used to Describe Continuous Systems", NASA Symposium on Transient Loads and Response of Space Vehicles, NASA-Langley Research Center, Nov. 7-8, 1967.

3. Archer, John, Journal of the "Structural Division", proceedings of the American Society of Civil Engineers (Aug. 1963) pp. 161.

4. Krishna Murthy, A. V., "A Lumped Inertia Force Method for Vibration Problems", The Aeronautical Quarterly (May 1966) pp. 127.

5. Rocke, R. D., "Transmission Matrices and Lumped Parameter Models for Continuous Systems", Ph.D. Thesis, California Institute of Technology (June 1966).

6. Timoshenko, S., "Vibration Problems in Engineering", D. Van Nostrans Company, Inc., New York (1955) pp. 297-323.

7. Voltera, E., "Dynamics of Vibrations", Charles E. Merrill Books, Inc., Columbus, Ohio (1965) pp. 257-272, 293-310.

8. Pestel, E. C. and Leckie, F. A., "Matrix Methods in Elastomechanics", McGraw Hill Book Company, Inc., New York (1963) pp. 32-35, 221-223, 227-233.

9. Thompson, W. T., "Vibration Theory and Applications", Prentice-Hall, Inc., New Jersey (1965) pp. 251-253, 99-102.

10. Jolley, L. B. W., "Summation of Series", Dover Publications, Inc., New York.

CHAPTER VIII

VITA

Suresh Kumar Tolani was born on January 15, 1946 in Calcutta, India. He received his primary and secondary education in New Delhi, India. He received a Bachelor of Engineering degree in Mechanical Engineering from Sardar Patel University in Anand, Gujerat State, India.

He has been enrolled in the graduate school of the University of Missouri - Rolla since September 1968 and has held a teaching assistantship for the period January 1969 to May 1969 and the N.S.F. Scholarship for the period June 1969 to November 1969. He is currently working towards his Ph.D. degree on an N.S.F. sponsored project at the University of Missouri - Rolla.